BBA - Molecular and Cell Biology of Lipids 1870 (2025) 159621

Contents lists available at ScienceDirect

BBA - Molecular and Cell Biology of Lipids

journal homepage: www.elsevier.com/locate/bbalip

Lipidome plasticity in medium- and long-chain fatty acid oxidation disorders: Insights from dried blood spot lipidomics☆

Inês M.S. Guerra [a,b], Hugo Rocha [c,d], Sónia Moreira [e,f], Ana Gaspar [g], Ana C. Ferreira [h], Helena Santos [i], Esmeralda Rodrigues [j], Paulo Castro-Chaves [j], Tânia Melo [a,b], Laura Goracci [k], Pedro Domingues [b], Ana S.P. Moreira [a,b,*], M. Rosário Domingues [a,b,*]

[a] CESAM - Centre for Environmental and Marine Studies, Department of Chemistry, University of Aveiro, Campus Universitário de Santiago, 3810-193 Aveiro, Portugal
[b] Mass Spectrometry Center, LAQV-REQUIMTE, Department of Chemistry, University of Aveiro, Campus Universitário de Santiago, 3810-193 Aveiro, Portugal
[c] Newborn Screening, Metabolism and Genetics Unit, Human Genetics Department, National Institute of Health Doutor Ricardo Jorge, 4000-053 Porto, Portugal
[d] Department of Pathological, Cytological and Thanatological Anatomy, School of Health, Polytechnic Institute of Porto, 4200-072 Porto, Portugal
[e] Reference Center for Hereditary Metabolic Diseases, Centro Hospitalar e Universitário de Coimbra, 3000-075 Coimbra, Portugal
[f] European Reference Network for Hereditary Metabolic Diseases – MetabERN, Portugal
[g] Inherited Metabolic Diseases Reference Centre, Lisboa Norte Hospital University Centre, Lisboa, Portugal
[h] Inherited Metabolic Diseases Reference Center, Unidade Local de Saúde de São José, University Medical Centre of Lisbon, Portugal
[i] Inherited Metabolic Diseases Reference Centre, Vila Nova de Gaia Hospital Centre, Vila Nova de Gaia, Portugal
[j] Inherited Metabolic Diseases Reference Centre, São João Hospital University Centre, Porto, Portugal
[k] Department of Chemistry, Biology and Biotechnology, University of Perugia (Perugia), Italy

ARTICLE INFO

Keywords:
Lipid metabolism disorders
Lipids
Microsampling
Whole blood
Liquid chromatography
Mass spectrometry

ABSTRACT

Fatty acid (FA) oxidation disorders (FAOD) are characterized by accumulation of specific acylcarnitines (CAR) and FA and can lead to potentially severe complications. In this study, dried blood spots (DBS) combined with LC-MS lipidomics analysis were used to assess lipidome plasticity in medium-chain acyl-CoA dehydrogenase deficiency (MCADD), long-chain hydroxyacyl-CoA dehydrogenase deficiency (LCHADD), and very long-chain acyl-CoA dehydrogenase deficiency (VLCADD), compared to control (CT) individuals, for screening potential prognostic biomarkers.

Statistically significant variations were found in CAR, biomarkers for FAOD diagnosis, but other lipid species showed variations depending on the FAOD. Common changes in all FAOD included a few phosphatidylcholine (PC) lipid species, notably an up-regulation of LPC 16:1, possibly associated with a higher risk of cardiovascular disease (CVD). In LCHADD and VLCADD, an up-regulation of odd-chain PC (PC 33:0, PC 35:4 and PC 37:4) was observed. VLCADD exhibited higher levels of odd-chain TG, while LCHADD showed an up-regulation of ceramide (Cer 41:2;O2). The increase in the Cer class has been found to be associated with neurodegeneration and may contribute to the risk of developing this condition in LCHADD. An upregulation of ether-linked PC lipid species, including plasmenyl (known as endogenous antioxidants), was observed in MCADD, possibly as a response to increased oxidative stress reported in this disorder.

Overall, DBS combined with lipidomics effectively pinpoints the lipid plasticity in FAOD, highlighting potential specific biomarkers for disease prognosis that warrant further validation for their association with the development of FAOD comorbidities.

1. Introduction

Fatty acid β-oxidation disorders (FAOD) are a group of rare inborn metabolic errors caused by defects in the mitochondrial fatty acid β-oxidation (FAO). The most prevalent FAOD include medium-chain acyl-CoA dehydrogenase deficiency (MCADD), long-chain hydroxy

☆ This article is part of a special issue entitled: 'ICBL2023' published in BBA - Molecular and Cell Biology of Lipids.

* Corresponding authors at: CESAM - Centre for Environmental and Marine Studies, Department of Chemistry, University of Aveiro, Campus Universitário de Santiago, 3810-193 Aveiro, Portugal.
E-mail addresses: ana.moreira@ua.pt (A.S.P. Moreira), mrd@ua.pt (M.R. Domingues).

https://doi.org/10.1016/j.bbalip.2025.159621
Received 1 August 2024; Received in revised form 14 April 2025; Accepted 29 April 2025
Available online 1 May 2025

acyl-CoA dehydrogenase deficiency (LCHADD), and very long-chain acyl-CoA dehydrogenase deficiency (VLCADD). Alterations at the level of acylcarnitines (CAR) with specific fatty acyl chains are used as biomarkers for diagnosis of each FAOD [1–3]. The inefficient fatty acid (FA) mitochondrial β-oxidation, together with accumulation of specific CAR and FA (of medium-chain in MCADD, long-chain 3-hydroxy in LCHADD, and long-chain in VLCADD), if not controlled, can lead to life-threatening clinical phenotypes [4–7]. Similar symptoms have been described for FAOD, such as acute hypoketotic hypoglycemia and encephalopathy episodes. However, other symptoms and comorbidities, such as cardiomyopathy and myopathy, are specific described for LCHADD and VLCADD, and the cardiac arrhythmias for long-chain FAOD and for few MCADD cases [8–15]. Only LCHADD patients present progressive neuropathy and retinopathy [3,16].

The therapeutic approach to manage FAOD is primarily focused on balancing energy deprivation and preventing the accumulation of toxic intermediates resulting from these metabolic defects [17]. Treatment strategies vary based on the patient's symptomatic or asymptomatic status, and the FAOD subtype [6]. In general, patients should avoid long fasting periods. Patients with long-chain FAOD (such as VLCADD and LCHADD) should also limit long-chain FA intake, follow a low-fat diet, and take supplements of medium-chain triacylglycerols containing C8 FA (MCT-C8). Additional therapeutic strategies, including anaplerotic therapy with triheptanoin may be employed. Triheptanoin, a triglyceride composed of three odd-chain C7 fatty acids (MCT-C7), can also serve as an alternative to MCT-C8 supplementation [17]. As energy supply depends on FAO, supplementing with carbohydrates may be required when glucose levels are low [18].

The accumulation of specific CAR and FA, as well as the dietary therapy and MCT supplementation (in the case of long-chain FAOD), can disrupt lipid homeostasis [3]. In addition, the accumulation of specific CAR and FA can contribute to enhancing cell oxidative stress, causing lipid peroxidation and ultimately inducing deregulation in lipid homeostasis and alteration of cellular lipid profile [4]. Besides the alterations in CAR and FA profiles, published works reported the variation in other lipid classes in MCADD, VLCADD, and LCHADD [19]. Lipidomics and metabolomics studies have reported changes at the level of CAR and other complex lipids, such as glycerophospholipids, sphingolipids, and glycerolipids [19–35]. A decrease in ether-linked lipids, namely phosphatidylcholine (PC) plasmalogens, known as endogenous antioxidants, was reported in the plasma of MCADD patients and associated with a possible increase in oxidative stress [19]. Alterations in the profile of the triacylglycerols (TG) containing saturated and monounsaturated FA (namely FA 14:0 and FA 16:0) were also reported in MCADD individuals [19]. These changes were linked to a potential risk of long-term development of cardiovascular disease, as reported for patients with obesity and type 2 diabetes mellitus [21–25]. Less is known regarding the changes in the complex lipids in LCHADD, but changes in the levels of TG, PC, phosphatidylethanolamine (PE), PC/PE ratio, sphingomyelins (SM), ceramides (Cer) and hexosylceramides (HexCer) were reported [26,28,29]. The authors hypotheses that the altered sphingolipid profile in LCHADD patients may be a long-term risk factor to the neurodegenerative symptoms of these patients [28], as increase in sphingolipids have been associated with neurodegenerative disorder [36,37]. In VLCADD patients, a higher content of lysophospholipids containing FA with 14 carbons was pointed as potentially contributing to the pro-inflammatory state of this disorder [32]. Increased levels of PC, ether-linked PC, and TG, together with lower content of ether-linked PE (with 36 and 38 total carbons in FA chains) were also observed in human VLCADD fibroblasts [28]. Thus, a disruption of lipid homeostasis and profile can have a significant impact on the onset and progression of FAOD [38–40]. The analysis of the specific variation of the lipidome may enable the identification of potential biomarkers for prognosis, as well as for valuating disease progression and assessing treatment effects [41,42].

The research on FAOD lipidome was focused on the analysis of plasma, fibroblasts, and dried blood spots (DBS) samples [3]. Recently, the use of DBS has attracted attention, and when combined with lipid analysis, it is considered highly advantageous for chronic diseases surveillance [43,44]. DBS sampling is a patient-centric approach to healthcare, as it is minimally invasive, requiring small blood volumes, and enabling easier sample collection. This makes DBS ideal for frequent follow-up, improving patient compliance and quality of life. DBS is already applied routinely for newborn screening and FAOD diagnosis, but it is limited to CAR quantification in FAOD patients. In this work, we aimed to use DBS combined with lipidomic analysis to access the whole blood lipid plasticity of MCADD, VLCADD, and LCHADD compared to control (CT) individuals, screening potential prognosis biomarker candidates.

2. Material and methods

2.1. Dried blood spot (DBS) samples

Whole blood from a total of 25 participants, including 10 controls (CT), 5 medium-chain acyl-CoA dehydrogenase deficiency (MCADD) patients, 5 very long-chain acyl-CoA dehydrogenase deficiency (VLCADD), and 5 long-chain hydroxy acyl-CoA dehydrogenase deficiency (LCHADD) patients, were collected by a heal/fingerpick on multiple 1.3 cm DBS circles of PerkinElmer ® 226 filter paper cards and stored at −20 °C until the total lipid extraction. The samples were divided into 4 groups: CT (subjects with 1 month to 28 years old, 4 females and 6 males), MCADD (subjects with 9 days to 10 years old, 4 females and 1 male), VLCADD (subjects with 3 to 22 years old, 2 females and 4 males) and LCHADD (subjects with 6 months to 28 years old, 2 females and 3 males). Data collected for each patient are summarized in Supplementary Table S1.

2.2. DSB total lipid extraction

Total lipids were extracted from each DBS using the Bligh & Dyer method [45]. For this, 8 circles of 3.2 mm, punched from the DBS circles, were placed in Pyrex extraction tubes. To each tube, 1 mL of Milli-Q water and 3.75 mL of dichloromethane: methanol (1:2, v/v) were added and vortexed for 1 min. Then, each tube was incubated on ice for 30 min under agitation (75 rpm) using an orbital shaker (Stuart Reciprocating Shaker SSL2, Stuart, UK), vortexing every 5 min. After 30 min, 1.25 mL of dichloromethane and 1.25 mL of Milli-Q water were added to each tube and vortexed for 1 min between each addition. The tubes were centrifuged at 2000 rpm for 10 min, and the lower organic phase was collected into a new glass tube. Then, 1.88 mL of dichloromethane was added to the aqueous phase, and the tubes were vortexed for 1 min. The tubes were then re-centrifuged under the same conditions to separate the aqueous phase from the remaining organic phase. The organic phase was collected into the previous glass tube, dried under a stream of nitrogen gas, and re-dissolved in dichloromethane. The total lipid extracts were transferred to amber vials, dried, and stored at −80 °C until further analysis.

2.3. Phospholipid quantification by phosphorus measurement

The quantification of total phospholipids (PL) recovered after extraction was performed through phosphorus (P) measurement, following a modified Bartlett and Lewis method [46], as previously described [19]. For that, the total lipid extracts were dissolved in 200 μL of dichloromethane, and a volume of 10 μL was transferred in duplicate to a glass tube previously washed with 5 % nitric acid. The solvent was dried using a nitrogen stream, and then 125 μL of 70 % perchloric acid was added to each tube. The samples were incubated in a heating block (Stuart, U.K.) at 180 °C for 1 h. After cooling to room temperature, 825 μL of Milli-Q water, 125 μL of ammonium molybdate (25 g L^{-1} prepared in Milli-Q water), and 125 μL of ascorbic acid (100 g L^{-1} prepared in

Milli-Q water) were added to each sample, with vortex mixing between each addition. The samples were then incubated in a water bath at 100 °C for 10 min, followed by immediate cooling in a cold-water bath. The absorbance was measured at 797 nm using a Multiskan GO1.00.38 Microplate Spectrophotometer (Thermo Scientific, Hudson, NH, USA) controlled by SkanIT software, version 3.2 (Thermo Scientific). The phosphorus content of each extract was determined using a calibration curve prepared by performing the same procedure (excluding the heating block step) with standards containing 0.1 to 2 μg of phosphorous, prepared from a sodium dihydrogen phosphate dihydrate solution (100 μg mL^{-1} of P). The total amount of phospholipids was estimated by multiplying the phosphorus amount by 25 [47].

2.4. Characterization of the total lipidome profile by reverse phase liquid chromatography coupled to high-resolution tandem mass spectrometry (C18 LC-MS/MS)

The total lipid extract from DBS samples was analyzed by reverse-phase liquid chromatography coupled to high-resolution tandem mass spectrometry (C18 LC-MS/MS) using an Ultimate 3000 Dionex (Thermo Fisher Scientific, Bremen, Germany) equipped with an Ascentis® Express 90 Å C18 column (Sigma-Aldrich®, 2.1 × 100 mm, 2.7 μm) coupled to a Q-Exactive® hybrid quadrupole Orbitrap mass spectrometer (Thermo Fisher Scientific, Bremen, Germany). For this analysis, the total lipid extracts obtained from DBS samples were resuspended in dichloromethane to achieve a phospholipid (PL) concentration of 1 μg PL μL^{-1}. A volume of 5 μL of a mixture containing 10 μL of lipid extract (previously resuspended in dichloromethane; 1 μg PL μL^{-1}), 82 μL of a solvent system of isopropanol:methanol (1:1, *v*/v), and 8 μL of a mixture of phospholipid standards (1,2-dimyristoyl-sn-glycero-3-phosphocholine - 0.04 μg, N-heptadecanoyl-D-erythro-sphingosylphosphorylcholine - 0.04 μg, 1,2-dimyristoyl-snglycero-3-phosphoethanolamine - 0.04 μg, 1-nonadecanoyl-2-hydroxy-sn-glycero-3phosphocholine - 0.04 μg, 1,2-dipalmitoyl-sn-glycero-3-phosphoinositol - 0.08 μg, 1′,3′-bis[1,2-dimyristoyl-sn-glycero-3-phospho]-glycerol - 0.16 μg; 1,2-dimyristoyl-snglycero-3-phosphoglycerol - 0.024 μg, N-heptadecanoyl-D-erythro-sphingosine - 0.08 μg, 1,2-dimyristoyl-sn-glycero-3-phospho-L-serine −0.08 μg; 1,2-dimyristoyl-sn-glycero3-phosphate - 0.16 μg) was injected, for each sample, into the column at 50 °C and at a flow rate of 260 μL min^{-1}. Mobile phase A consisted of Milli-Q water/acetonitrile (ACN) (40/60 %) with 10 mM ammonium formate and 0.1 % formic acid, while mobile phase B comprised isopropanol/ACN (90/10 %) with 10 mM ammonium formate and 0.1 % formic acid. The elution started with 32 % of mobile phase B, followed by the following gradient: 45 % B (1.5 min), 52 % B (4 min), 58 % B (5 min), 66 % B (8 min), 70 % B (11 min), 85 % B (14 min), 97 % B (18 min), 97 % B (25 min), 32 % B (25.01 min, followed by an 8-min re-equilibration period before the next injection). The mass spectrometer operated simultaneously in positive mode (electrospray voltage 3.0 kV) and negative mode (electrospray voltage 2.7 kV). The gas flow was 35 U, the auxiliary gas was 3 U, the capillary temperature was 320 °C, the S-lenses RF was 50 U, and the probe temperature was 300 °C. Data acquisition was performed in full scan mode with a high resolution of 70,000 and automatic gain control (AGC) target of 3×10^6, in an *m/z* range of 200–1600, with 2 micro scans, and a maximum injection time (IT) of 100 ms. Tandem mass spectra (MS/MS) were obtained with a resolution of 17,500, AGC target of 1×10^5, 1 micro scan, and a maximum IT of 100 ms. The cycles consisted of a full-scan mass spectrum and 10 data-dependent MS/MS scans, which were repeated continuously throughout the experiments with a dynamic exclusion of 30 s and an intensity threshold of 8×10^4. The normalized collision energy (CE) ranged between 20, 24, and 28 eV in the negative mode and 25 and 30 eV in the positive mode. Data acquisition was performed using the Xcalibur data system (V3.3, Thermo Fisher 6 Scientific, Bremen, Germany). The LC-MS data were processed using Lipostar software (Molecular Discovery Ltd., version 2.1.5) [7]. This software was used for raw data import, peak detection, and identification. Lipid assignment and identification were performed against a database created from the LIPID MAPS structure database (version November 2023). The database was fragmented using the DB Manager Module of Lipostar, following Lipostar fragmentation rules. The raw files were directly imported and aligned using the settings described by Lange *et al.* [8] Automatic peak picking was carried out with the SDA smoothing level set to low and a minimum signal-to-noise ratio of 3 and a signal filtering threshold of automatic in the positive mode and negative mode. Automatic isotope clustering settings were set to 0 ppm with a retention time tolerance of 0.2 min. The MS/MS filter was applied to retain only features with MS/MS spectra for identification. Lipid identification was based on the following parameters: a 5 ppm precursor ion mass tolerance and a 10 ppm product ion mass tolerance. An automatic approval process was applied to retain structures with a confidence level of 2–4 stars [7]. The areas of the identified and approved lipid species were then exported. For semi-quantitation, the peak areas of each lipid species were normalized by calculating the ratio against the sum of the areas.

2.5. Statistical analysis

Multivariate and univariate statistical analyses were performed using R version 4.3.1 [48] in RStudio version 2024.04.2 [49]. The area of lipid species (from LC–MS) was normalized by the total area sum and transformed using log transformation (base 10) [50], and further normalized using EigenMS [51]. The R packages FactoMineR [52] and factoextra [53] were used to perform principal component analysis (PCA). Heatmaps were created from autoscaled data using the R package pheatmap [54], using "Euclidean" as the clustering distance, and "ward.D" as the clustering method. Data normality and variance homogeneity were assessed using Shapiro-Wilk and Levene's tests, respectively. Based on these tests, data were analyzed using ANOVA if assumptions were met, or the Kruskal-Wallis test if not. Significant differences identified by ANOVA were further examined with Tukey's HSD test, while Dunn's test was used for the Kruskal-Wallis post hoc comparisons. *P*-values were corrected for multiple testing using the Benjamin−Hochberg method for the false discovery rate (FDR, *q*-values). All univariate analyses were performed using the r package rstatix [55] with a significance threshold of $p < 0.05$. All graphics and boxplots were created using the R package ggplot2 [56].

3. Results

3.1. Total lipidome profile of control (CT) individuals, MCADD, VLCADD, and LCHADD patients using C18 LC–MS/MS

The lipid profile of DBS samples from MCADD, VLCADD, and LCHADD patients, and control (CT) individuals, was analyzed using a high-resolution C18-RP-LC–MS and MS/MS. A total of 266 different lipid species (*m/z* values) were identified (Supplementary Table S2), belonging to 12 lipid classes, including acylcarnitines (CAR); phosphatidylcholine (PC), comprising diacyl, lyso-PC (LPC), alkyl-acyl (indicated with the prefix 'O-' or also named as plasmanyl) and alkenyl-acyl species (indicated with prefix 'P-' or also named as plasmenyl); phosphatidylethanolamine (PE), including diacyl, lyso-PE (LPE), alkyl-acyl and alkenyl-acyl species; phosphatidylinositol (PI); phosphatidylserine (PS), including diacyl, alkyl-acyl and alkenyl-acyl species; sphingomyelin (SM); ceramide (Cer); hexosylceramide (HexCer); dihexosylceramide (Hex_2Cer); cholesteryl ester (CE); diacylglycerol (DG); and triacylglycerol (TG). For most of the identified lipid species, the fatty acyl composition was determined, using MS/MS data, as shown in Supplementary Table S2. The lipid species were semi-quantified, and the statistical analysis was performed to assess the discrimination between the four groups considering two datasets: 1) acylcarnitines (CAR), glycerophospholipids (PC, LPC, PE, LPE, PI, PS) and sphingolipids (SM, Cer, HexCer and Hex_2Cer) and 2) glycerolipids (DG and TG) and sterol

lipids (CE).

3.2. Comparison of acylcarnitines, glycerophospholipids, and sphingolipids profile of MCADD, VLCADD, LCHADD, and control (CT) individuals

The acylcarnitines, glycerophospholipids, and sphingolipids profiles were compared between FAOD (MCADD, VLCADD, and LCHADD) and controls (CT) groups using a multivariate and univariate analysis. To reduce the dimensionality of the data and to visualize sample clustering, a principal component analysis (PCA) was performed (Fig. 1). The PCA score plot showed clear discrimination between MCADD, long-chain FAOD (LCHADD and VLCADD), and CT groups, describing 54.2 % of the total variance with the contribution of Dimension 1 (Dim1, 33.4 %) and Dimension 2 (Dim2, 20.8 %). The CT group (plotted at negative values of Dim2) was well separated from the three FAOD groups. A clear separation between the medium-chain (MCADD) and long-chain FAOD (VLCADD and LCHADD) groups was visible along Dim1. However, an overlap of the 95 % confidence ellipse was observed between VLCADD and LCHADD groups. According to the loading values, Dim1 significant contributors were 5 CAR, 7 PC, 1 LPC, 1 PE, and 2 PI (Supplementary Fig. S1). The main contributors for the Dim2 discrimination were 4 CAR, 7 PC, 3 LPC, 1 LPE, and 1 Cer (Supplementary Fig. S2).

Univariate analysis showed that 134 out of 173 identified lipid species were significantly different between the four conditions with a q-value<0.05 (Supplementary Table S3). The results of the ANOVA test were used to select the top 50 lipid species with the lowest q-values (q-values <0.001) to create a two-dimensional hierarchical clustering heatmap (Fig. 2). These 50 lipid species, which contribute most to the differentiation of DBS samples from CT, MCADD, VLCADD and LCHADD groups, included 7 acylcarnitines (CAR), 34 glycerophospholipids (20 PC, 3 ether-linked PC, 3 LPC, 1 ether-linked LPC, 1 PE, 1 ether-linked PE, 1 LPE, 3 PI, and 1 ether-linked PS), and 9 sphingolipids (5 SM, 3 Cer and 1 HexCer). The samples were clustered independently into two groups, on the top of the hierarchical dendrogram, with CT (green) on the left side and FAOD groups, MCADD (purple), LCHADD (orange), and VLCADD (pink), on the right side. The FAOD cluster showed a clear separation between MCADD and long-chain FAOD (LCHADD and VLCADD).

The clustering of the lipid species with respect to their similarity variation is shown on the dendrogram on the left side of the heatmap (Fig. 2). The first upper cluster included a total of 15 lipid species, of which 10 lipid species (CAR 12:1, CAR 14:0, CAR 18:2, PI 36:1, PI 36:2, PI 34:2, SM 41:2;O2, Cer 41:2;O2 and HexCer 41:1;O2) were decreased in the MCADD when compared to LCHADD, VLCADD and CT groups. On the other hand, 5 lipid species (CAR 18:1, PC 34:2, PC 36:2, PE 36:2, and LPE 18:2) were downregulated in all FAOD (MCADD, LCHADD, and VLCADD) compared to CT group. The second cluster in the first level of the dendrogram included 35 lipid species, of which 12 lipid species were increased in MCADD group (CAR 8:0, PC 22:0, PC 38:1, PC 38:2, PC 37:2, PC 37:1, PC 39:6, PC 40:3, PC 40:7, PC O-40:6/PC P-40:5, PC O-38:6/ PC P-38:5, and LPC 20:5). In addition, 11 lipid species (CAR 14:1, PC 31:0, PC 33:0, PC 35:4, PC 37:4, PC 38:6, PC 40:6, PC 40:8, LPC O-17:1/LPC P-17:0, SM 37:1;O2 and SM 40:3;O2) were up-regulated in long-chain FAOD (LCHADD and VLCADD). Whereas, CAR 16:0;O, Cer 36:1;O2 and PS O-34:2/PS P-34:1 were only up-regulated in LCHADD group. The other 9 lipid species (PC 20:0, PC 30:0, PC 30:1, LPC 16:1, LPC 22:6, PE P-38:6, SM 36:0;O2, SM 36:1;O2 and Cer 42:0;O2) were up-regulated in all FAOD.

Additionally, the 16 most significant lipid species with the lowest q-values (ANOVA test followed by Tukey's test) were selected and presented in the boxplot (Fig. 3). These 16 lipid species include 5 CAR, 8 PC, 2 LPC, and 1 Cer. Up-regulation of CAR 8:0 and down-regulation of CAR 12:1 was only observed in MCADD patients compared to long-chain FAOD (LCHADD and VLCADD) and CT groups. On the other hand, CAR 14:1 showed higher abundance in long-chain FAOD compared to MCADD and CT groups. LCHADD patients revealed higher levels of CAR 16:0;O, compared to MCADD, VLCADD, and CT individuals. CAR 18:1 was lower in LCHADD, MCADD and VLCADD groups, compared to CT group. The PC 20:0, PC 39:6, PC 40:6, LPC 20:5, LPC 22:6 and Cer 36:1;O2 showed higher abundance in all FAOD groups (MCADD, VLCADD, and LCHADD) compared to CT. However, increased levels of PC 37:1, PC 38:1, and PC 38:2 were only observed in MCADD patients, when compared to the long-chain FAOD and CT individuals. In contrast, the VLCADD group showed a decrease in the relative abundance of PC 38:1 compared to MCADD and CT groups. An increase in PC 38:6 was observed for both long-chain FAOD (LCHADD and VLCADD).

The 50 most discriminant lipid species included 3 CAR lipid species (CAR 8:0, CAR 16:0; O and CAR 14:1) with specific variation to each FAOD (Table 1). The 50 most discriminant lipid species from the top 50 of the CAR, glycerophospholipids, and sphingolipids dataset presented variations according to each disorder, namely 10 lipid species showed the same trend in all FAOD compared to CT (Table 1). These included the up-regulation of 4 diacyl-PC (PC 20:0, PC 39:6, PC 40:6 and PC 40:8), 2 lyso-PC species (LPC 16:1, LPC 20:5 and LPC 22:6), 1 plasmenyl PE (PE P-38:6) and 1 ceramide (Cer 36:1;O2), and the down-regulation of 1 diacyl-PE (PE 36:2) and 1 lyso-PE (LPE 18:2). Specific variations were noticed for MCADD patients compared with the other individuals (LCHADD, VLCADD, and CT) (Table 1). These included an up-regulation of 1 CAR (CAR 8:0), 6 diacyl-PC (PC 37:1, PC 37:2, PC 38:1, PC 38:2, PC 40:3 and PC 40:7), and 2 ether-linked PC (PC O-38:6/PC P-38:5 and PC O-40:6/PC P-40:5), and a down-regulation of 4 CAR (CAR 12:1, CAR 14:0, and CAR 18:2), 1 plasmanyl PC (PC O-33:0), 1 PI (PI 34:2), 1 SM (SM 41:2;O2), 1 Cer (Cer 41:2;O2) and 1 HexCer (HexCer 41:1;O2). Some lipid species (10 of the top 50) showed the same variation trend in long-chain FAOD (LCHADD and VLCADD). Of these, a down-regulation of 1 diacyl-PC (PC 36:2), together with an up-regulation of 1 CAR (CAR 14:1), 5 diacyl-PC (PC 31:0, PC 33:0, PC 35:4, PC 37:4 and PC 38:6), 1 ether-linked lyso-PC (LPC O-17:1/LPC P-17:0), and 2 SM (SM 37:1;O2 and SM 40:3;O2) was observed in long-chain FAOD, when compared to MCADD and CT individuals. The LCHADD patients exhibited a specific up-regulation in CAR 16:0;O and Cer 41:2;O2 compared to the MCADD, VLCADD, and CT individuals. For VLCADD, a specific increase in CAR 12:1, CAR 14:0, and PI 36:2 and a decrease in PC 38:1 was observed compared to CT, LCHADD, and MCADD individuals.

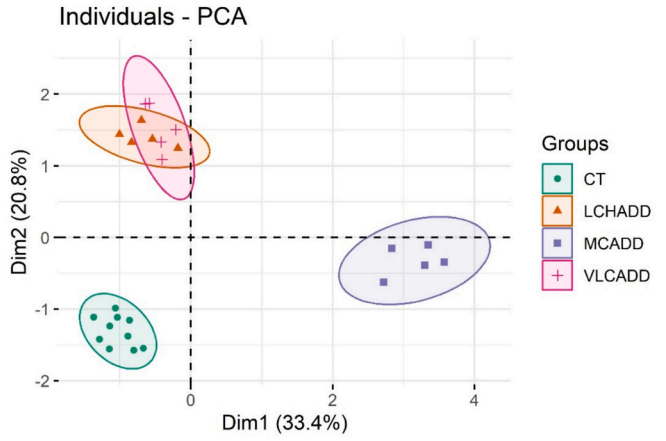

Fig. 1. Principal component analysis (PCA) score plot for total lipid extracts from DBS samples of medium-chain acyl-CoA dehydrogenase deficiency (MCADD), long-chain hydroxy acyl-CoA dehydrogenase deficiency (LCHADD), very long-chain acyl-CoA dehydrogenase deficiency (VLCADD) and controls (CT) individuals. The lipid dataset composed by acylcarnitines, glycerophospholipids, and sphingolipids obtained using a high-resolution C18-RP-LC–MS and MS/MS analysis was used as variables.

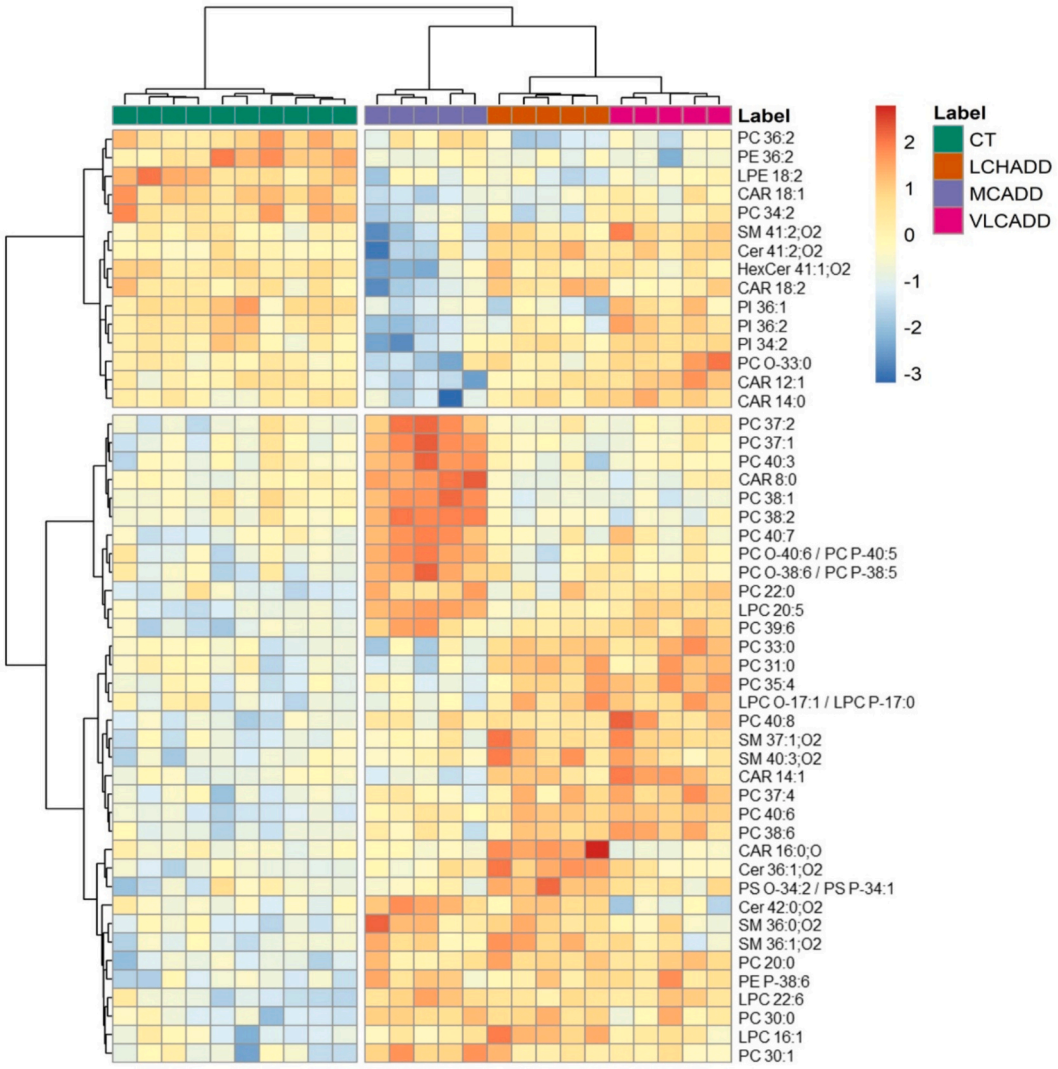

Fig. 2. Two-dimensional hierarchical clustering heatmap of the 50 most discriminative (q-values <0.001) acylcarnitines, glycerophospholipids, and sphingolipids lipid species among the CT, MCADD, LCHADD, and VLCADD groups. The relative abundance levels are shown on the red-yellow-blue scale, with numbers representing the fold difference from the overall mean. The red colour indicates high abundance, while blue indicates low abundance. Yellow represents null values. The clustering of the control and disease groups is represented by the dendrogram at the top, while the clustering of individual lipid species is represented by the dendrogram on the left. The lipid species are labelled as follows: AAAA xx:i (AAAA = lipid class abbreviation; xx = number of carbon atoms in FA; i = number of double bonds). The prefix 'O-' is used for plasmanyl species to indicate the presence of an alkyl ether substituent, whereas the prefix 'P-' is used for plasmenyl species to indicate the alk-1-enyl ether substituent. The abbreviations of lipid classes are as follows: CAR, acylcarnitines; Cer, ceramide; HexCer, hexosylceramide; LPC, lysophosphatidylcholine; LPE, lysophosphatidylethanolamine; PC, phosphatidylcholine; PE, phosphatidylethanolamine; PI, phosphatidylinositol; and SM, sphingomyelin; The fatty acyl chain compositions can be found in Supplementary Table S2.

3.3. Comparison of glycerolipids and sterol lipid profile of MCADD, VLCADD, LCHADD, and control (CT) individuals

The neutral lipidome, including TG, DG, and CE, was also compared between the four groups by multivariate analysis. A total variance of 70.4 % was described in the PCA score plot (Fig. 4), including the Dim1 with 41.6 % and the Dim2 with 28.8 %. The PCA score plot revealed a separation between CT, medium-chain (MCADD), and long-chain FAOD (VLCADD and LCHADD) groups. The CT group was scattered in the left region of the plot (negative values of Dim1), while FAOD (MCADD, VLCADD, and LCHADD) were scattered in the right region of the plot. The different disorders discriminate clearly from the CT group, but the 95 % confidence ellipse for the VLCADD and LCHADD groups overlapped. However, the MCADD was well separated from the long-chain FAOD (VLCADD and LCHADD) groups.

The univariate analysis revealed that 87 out of 99 neutral lipid species were significantly different between the four groups ($q < 0.05$) (Supplementary Table S4). The results of the ANOVA test were used to select the top 50 neutral lipid species with the lowest q-values ($q <$ 0.001) to create a two-dimensional hierarchical clustering heatmap (Fig. 5)). In the first level of the dendrogram at the top of the heatmap (Fig. 5), the CT (green) and MCADD (purple) groups were separated from the LCHADD (orange) and VLCADD (pink) groups. Regarding the variations in the neutral lipid species, the first cluster in the first level of the dendrogram included 12 TG species (mostly esterified with FA 16:0, FA 18:0, and FA 18:1) and 2 DG (most containing FA 16:0 and FA 18:1 in their composition) (Supplementary Table S2). All these 14 neutral lipid species were down-regulated in long-chain FAOD (LCHADD and VLCADD) individuals. The second cluster presented a total of 36 TG lipid species. Of these 36 TG lipid species (in the second level of the dendrogram), 18 TG lipid species esterified with saturated and monosaturated FA (such as FA 15:0, FA 16:0, FA 17:0, FA 18:0, FA 16:1, FA 17:1 and FA 18:1) were up-regulated in VLCADD group. The other 18 TG lipid species were separated in the third level of the dendrogram, of

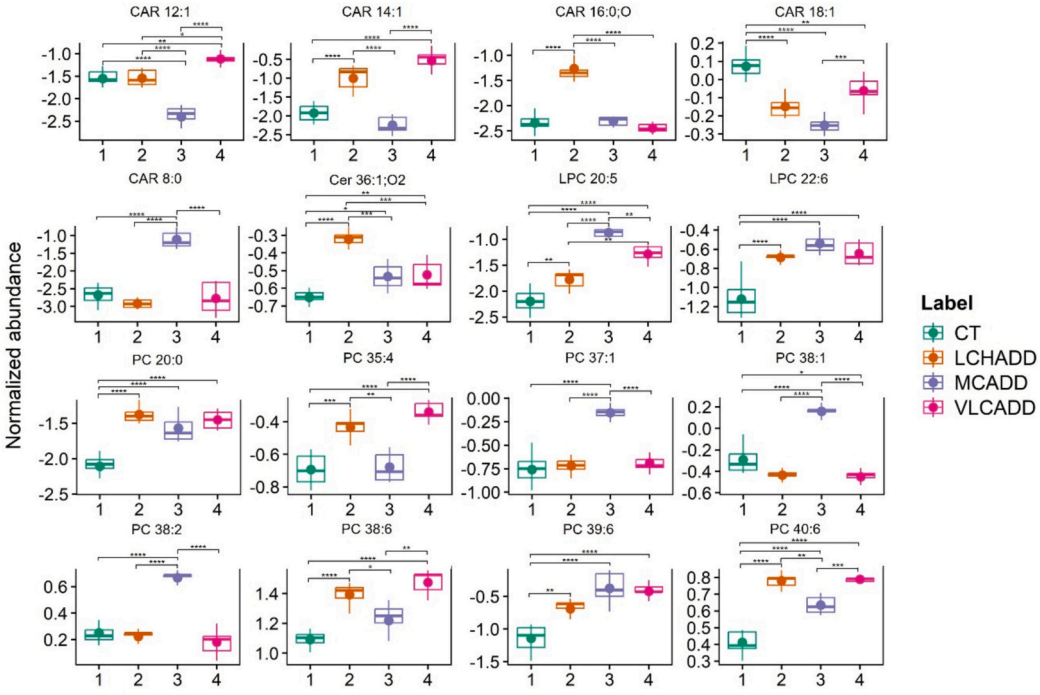

Fig. 3. Boxplots of the 16 most significant acylcarnitines, glycerophospholipids, and sphingolipids lipid species identified through univariate analysis between control (CT), long-chain hydroxy acyl-CoA dehydrogenase deficiency (LCHADD), medium-chain acyl-CoA dehydrogenase deficiency (MCADD), and very long-chain acyl-CoA dehydrogenase deficiency (VLCADD) individuals. Significant differences between the groups are identified by horizontal lines and marked as follows: * $q < 0.05$, ** $q < 0.01$, *** $q < 0.001$ and **** $q < 0.0001$. The lipid species are labelled as follows: AAAA (xx: i) (AAAA = lipid class abbreviation; xx = the number of carbon atoms in FA(s); i = the number of double bonds). Abbreviations of the lipid classes: CAR, acylcarnitine; Cer, ceramide, LPC, lysophosphatidylcholine; PC, phosphatidylcholine; PE, phosphatidylethanolamine; PI, phosphatidylinositol.

which 8 TG lipid species were increased in MCADD and 10 TG were increased in long-chain FAOD.

A boxplot reporting the 16 most significant neutral lipid species with the lowest *q*-values (selected from the ANOVA noted by Tukey's test) is presented in Fig. 6. Among these 16 neutral lipid species, 9 TG species (TG 44:1, TG 52:6, TG 54:6_b, TG 54:7, TG 56:6, TG 56:7, TG 58:7, TG 58:8 and TG 58:9) were up-regulated and 1 TG (TG 52:2) was down-regulated in FAOD patients (MCADD, LCHADD and VLCADD) compared to CT individuals. In addition, long-chain FAOD (LCHAD and VLCADD) showed a decrease in the relative abundance of DG 36:2, TG 54:3, TG 56:3, TG 58:2 and TG 60:2, while TG 49:0 was increased in these two groups.

Among the top 50 of the neutral lipids, an up-regulation of 13 TG lipid species (TG 44:1, TG 52:5, TG 52:6, TG 54:6_b, TG 54:7, TG 56:6, TG 56:7, TG 58:7, TG 58:8, TG 58:9, TG 44:2, TG 54:5, and TG 42:1) and a downregulation of TG 52:2 was observed in all FAOD (MCADD, LCHADD, and VLCADD) compared to CT individuals (Table 1). For long-chain FAOD (LCHADD and VLCADD), a down-regulation of DG 36:2 and 7 TG lipid species (TG 54:2, TG 54:3, TG 56:2, TG 58:2, TG 58:3, TG 56:3 and TG 60:2), together with an up-regulation of other 8 TG (TG 46:3, TG 49:0, TG 49:2, TG 50:3, TG 50:4, TG 51:0, TG 51:1 and TG 51:4) was observed in these patients compared to CT and MCADD individuals. LCHADD patients exhibited a specific up-regulation in TG 50:0 and a down-regulation in TG 54:4, compared to CT, MCADD, and VLCADD. VLCADD patients presented a specific up-regulation of 10 TG species (TG 43:0, TG 42:0, TG 45:0, TG 45:1, TG 45:2, TG 47:0, TG 47:1, TG 47:2, TG 49:1, and TG 49:3). In addition, MCADD patients showed increased levels of DG 36:4 and 5 TG lipid species (TG 56:3, TG 56:4, TG 58:3, TG 58:2 and TG 60:2), together with decreased levels of TG 49:0, TG 49:1 and TG 51:1.

4. Discussion

Mitochondrial fatty acid β-oxidation disorders (FAOD) are inborn errors of metabolism characterized by defects in specific enzymes/transporters involved in mitochondrial fatty acid β-oxidation, leading to accumulation of specific CAR and their FA precursors [19,28,29,32]. Thus, a panel of CAR is well established in newborn screening diagnosis and clinical routine follow-up based on using dried blood spots (DBS) and mass spectrometry analysis (Table 2) [3]. The newborn screening allows an early therapeutic approach to manage these disorders. FAOD patients need to avoid long fasting periods with frequent feeding and require careful management during acute illness [57,58]. In long-chain FAOD (LCHADD and VLCADD), a lipid-restricted diet is also needed, with limited consumption of dietary lipids (containing long-chain fatty acids) and supplementation with MCT containing medium-chain FA [58]. Despite dietary therapy, few studies have reported that alterations in the lipidome can occur in FAOD and may be linked to the development of associated comorbidities (Table 2) [3,19]. However, the changes in the FAOD lipidome are underexplored, and further clarification of their long-term impacts is necessary, as changes in the lipidome have been associated with various diseases, including cardiovascular disease (CVD) [41,42]. Therefore, in our work, we used a lipidomic approach to profile the whole blood collected in DBS from FAOD (MCADD, LCHADD, and VLCADD) and control (CT) individuals. The lipidomic data were analyzed using multivariate and univariate analysis. The profile in complex lipids was separated into two datasets: 1) CAR, glycerophospholipids, and sphingolipids, and 2) neutral lipids, including glycerolipids (triacylglycerols and diacylglycerols) and sterol lipids.

The PCA and clustering analysis of the top 50 of the most discriminative lipid species from CAR, glycerophospholipids, and sphingolipids dataset revealed that the three FAOD groups differed from the CT group (Figs. 1 and 4). However, long-chain FAOD (LCHADD and VLCADD)

Table 1
Significant variations, considering the 50 most discriminant lipid species (*q*-values <0.001) within each dataset, that were identified as common for FAOD and observed in MCADD, LCHADD, and VLCADD. Lipid species with the same variation trend (increase or decrease) in long-chain FAOD (LCHADD and VLCADD) are highlighted in **bold**. The acylcarnitines (CAR) lipid species used as biomarkers in newborn screening are underlined.

Lipid class	[a]Common to FAOD (MCADD, LCHADD, and VLCADD)	[b]Observed in MCADD	[c]Observed in LCHADD	[d]Observed in VLCADD
Variations considering acylcarnitines, glycerophospholipids, and sphingolipids dataset				
CAR		↑ CAR 8:0 ↓ (CAR 12:1, CAR 14:0 and CAR 18:2)	↑ (CAR 16:0;O and **CAR 14:1**)	↑ (CAR 12:1, CAR 14:0 and **CAR 14:1**)
PC	↑ (PC 20:0, PC 39:6, PC 40:6 and PC 40:8)	↑ (PC 37:1, PC 37:2, PC 38:1, PC 38:2, PC 40:3, PC 40:7, PC O-38:6/ PC P-38:5 and PC O-40:6/PC P-40:5) ↓ (PC O-33:0)	↑ (**PC 31:0, PC 33:0, PC 35:4, PC 37:4** and **PC 38:6**) ↓ **PC 36:2**	↑ (**PC 31:0, PC 33:0, PC 35:4, PC 37:4** and **PC 38:6**) ↓ **PC 36:2**
LPC	↑ (LPC 16:1, LPC 20:5 and LPC 22:6)		↑ **LPC O-17:1/ LPC P-17:0**	↑ **LPC O-17:1/ LPC P-17:0**
PE	↑ (PE P-38:6) ↓ (PE 36:2)			
LPE	↓ LPE 18:2			
PI		↓ PI 34:2		
SM		↓ SM 41:2;O2	↑ (**SM 37:1;O2** and **SM 40:3; O2**)	↑ (**SM 37:1;O2** and **SM 40:3; O2**)
Cer HexCer	Cer 36:1;O2	↓ Cer 41:2;O2 ↓ HexCer 41:1; O2	↑ Cer 41:2;O2	
Variations considering diacylglycerols, triacylglycerols, and cholesterol esters dataset				
DG		↑ DG 36:4	↓ **DG 36:2**	↓ **DG 36:2**
TG	↑ (TG 44:1, TG 52:5, TG 52:6, TG 54:6_b, TG 54:7, TG 56:6, TG 56:7, TG 58:7, TG 58:8, TG 58:9, TG 44:2, TG 54:5 and TG 42:1) ↓ TG 52:2	↑ (TG 56:3, TG 56:4, TG 58:2, TG 58:3 and TG 60:2) ↓ TG 49:0, TG 49:1 and TG 51:1	↑ (**TG 46:3, TG 49:0, TG 49:2** TG 50:0, **TG 50:3, TG 50:4, TG 51:0, TG 51:1** and **TG 51:4**) ↓ (**TG 54:2, TG 54:3,** TG 54:4, **TG 56:2, TG 58:2, TG 58:3, TG 56:3** and **TG 60:2**)	↑ (TG 42:0, TG 43:0, TG 45:0, TG 45:1, TG 45:2, **TG 46:3,** TG 47:0, TG 47:1, TG 47:2, TG 49:1, **TG 49:0, TG 49:2** TG 49:3, **TG 50:3, TG 50:4, TG 51:0, TG 51:1** and **TG 51:4**) ↓ (**TG 54:2, TG 54:3, TG 56:2, TG 58:2, TG 58:3, TG 56:3** and **TG 60:2**)

Lipid class abbreviations: CAR, acylcarnitine; Cer, ceramide; HexCer, hexosylceramide; LPC, lysophosphatidylcholine; LPE, lysophosphatidylethanolamine; PC, phosphatidylcholine; PE, phosphatidylethanolamine; PI, phosphatidylinositol; SM, sphingomyelin; DG, diacylglycerol; TG, triacylglycerol.

[a] Comparation of FAOD vs CT.
[b] Comparation of MCADD vs CT, VLCADD, and LCHADD.
[c] Comparation of LCHADD vs CT, MCADD, and VLCADD.
[d] Comparation of VLCADD vs CT, MCADD, and LCHADD.

cluster more close compared with MCADD or CT groups (Fig. 1). The 50 most discriminant lipid species included 3 CAR lipid species (CAR 8:0, CAR 16:0;O and CAR 14:1) with specific variation to each FAOD (Table 1), in line with the already known as FAOD biomarkers (Table 2). MCADD patients exhibited a specific increase in CAR 8:0 (Table 1), which is used as a biomarker for MCADD diagnosis in newborn screening (Table 2) [3]. The observed up-regulation of CAR 16:0;O, used in LCHADD diagnosis (Table 2), was consistent with previous studies [6–13]. CAR 14:1 was specifically up-regulated in long-chain FAOD (LCHADD and VLCADD). An increased level in the CAR 14:1 was previously reported for LCHADD and VLCADD patients [20,32]. Our data also revealed a significantly higher up-regulation of CAR 14:1 in VLCADD patients compared to LCHADD, which is in agreement with the fact that CAR 14:1 is used as a diagnostic biomarker for VLCADD, but not for LCHADD (Table 2) [20,59,60]. Overall, the CAR lipid species from the clinical panel for FAOD diagnosis were detected in our work, demonstrating that DBS combined with lipidomic analysis identifies the characteristics CAR profile used for FAOD diagnosis and could be used fordisease surveillance.

The complex lipids from the top 50 of the CAR, glycerophospholipids, and sphingolipids dataset also included 10 lipid species that showed the same trend in all FAOD compared to CT. Of these, an up-regulation of PE P-38:6 was observed. Plasmenyl PE have been reported as endogenous antioxidants [61,62], and their increase levels may be beneficial for FAOD patients because plasmalogens can decrease oxidative stress [63] which was previously reported in FAOD patients [64–66]. A down-regulation in PE 36:2 was observed in the FAOD individuals, but its biological role is still unrevealed. The decrease in PE lipid class may be related to the increase in PC class, since several PC species were up-regulated in FAOD, as PE can be converted into PC lipids through the action of PE *N*-methytransferase (PEMT) in the Kennedy pathway [67]. The increase in PC/PE ratio was previously observed in long-chain FAOD (LCHADD and VLCADD) [28,29]. In all FAOD patients, an up-regulation of the LPC 16:1 compared to CT individuals was observed. In fact, a lower degree of unsaturation in LPC has been associated with atrial fibrillation [68], and increased LPC class has been also observed in hypertrophy cardiomyopathy (HCM) [69]. An increase in PC 40:6 and PC 40:8 was also observed in this study and common to all FAOD patients. Previously, increased PC 40:6 and PC 40:8 have been associated with a lower CVD events, such as atrial fibrillation, myocardial infraction and death [70]. The manifestation of CVD has been considered more prevalent in long-chain FAOD patients [7,71], wherefore the relevance of these lipid variations observed across all FAOD (MCADD, LCHADD, and VLCADD) warrants further investigation. The increase in LPC 22:6 may also be beneficial for patients with FAOD, as this LPC is known to have anti-inflammatory properties, as evaluated using RAW 264.7 cells [72].

Regarding the variations observed for MCADD patients, there was a decrease in SM 41:2;O2, in line with what was previously reported in the plasma of MCADD children [19], but it was not associated with any possible effect/comorbidity. Furthermore, MCADD patients showed higher levels of PC 38:2 (PC 16:0_22:2), esterified with FA 16:0, and the increase in FA 16:0 was previously reported in the plasma of MCADD patients [19]. Additionally, MCADD exhibited an up-regulation in ether-linked PC, specifically in PC O-38:6/PC P-38:5 and PC O-40:6/PC P-40:5, compared to the CT and long-chain FAOD individuals. As plasmenyl PC are known as endogenous antioxidants [61,62,73,74], the possible increase in plasmenyl PC lipid species may be a response to the increased oxidative stress, which has already been reported in MCADD [64,75–78].

Long-chain FAOD revealed a common trend in the variation of some lipid species. The up-regulation of the SM 37:1;O2 and SM 40:3;O2 was observed for long-chain FAOD when compared with MCADD and CT, and may be related with CVD risk, as increased levels of SM were observed in HCM [69]. Furthermore, long-chain FAOD (LCHADD and VLCADD) patients exhibited a down-regulation of PC 36:2 (PC

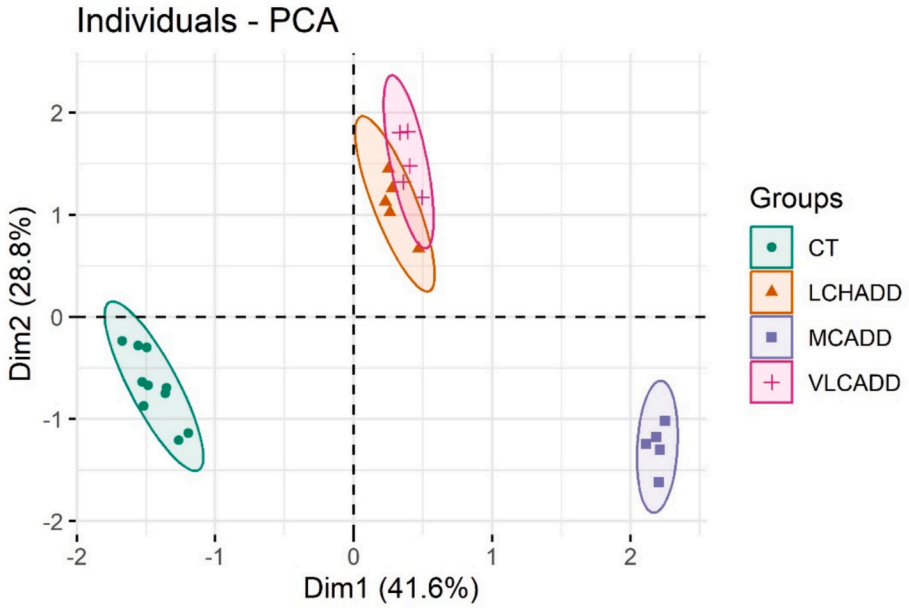

Fig. 4. Principal component analysis (PCA) score plot of total lipid extracts from DBS samples of medium-chain acyl-CoA dehydrogenase deficiency (MCADD), long-chain hydroxy acyl-CoA dehydrogenase deficiency (LCHADD), very long-chain acyl-CoA dehydrogenase deficiency (VLCADD) and controls (CT) individuals. The lipid dataset of neutral lipid species obtained using a high-resolution C18 LC–MS and MS/MS analysis was used as variables.

18:0_18:2), containing essential linoleic acid (FA 18:2 *n*-6). Decreased levels of FA 18:2 *n*-6 were previously reported in the plasma and red blood cells of LCHADD patients [35], and also in VLCAD$^{-/-}$ mice supplemented with MCT [30]. As mentioned by Lund *et al.* [35], it is not clear why FA 18:2 *n*-6 was decreased and possible adverse effects. The decrease in the lipid content FA 18:2 *n*-6 esterified to phospholipids can be related to the low-fat diet intake, as long-chain FAOD are typically managed with a low-fat diet. As low-fat diets are associated with reduced levels of FA 18:2 *n*-6 [79], it is plausible that this dietary approach could lower the abundance of this FA in the lipidome. However, it is important to highlight that FA 18:2 *n*-6 is an essential FA only obtained through dietary intake [80]. The decrease in FA 18:2 *n*-6 can have noteworthy implications, particularly for maintaining cell membrane structure, as this essential FA is also esterified into cell membrane phospholipids and thus can modulate membrane properties and cell/organ function [80,81]. Beyond its role on membrane integrity, FA 18:2 *n*-6 also plays a protective role against cardiovascular disease [82] and in LDL cholesterol levels [83]. Therefore, its deficiency may negatively impact health. Also, in this study, it was observed an up-regulation of the PC 33:0 (PC 15:0_18:0), PC 35:4 (PC 15:0_20:4) and PC 37:4 (PC 17:0_20:4) in long-chain FAOD patients (LCHADD and VLCADD). Both PC were esterified with odd-chain FA, such as pentadecanoic acid (FA 15:0) and heptadecanoic acid (FA 17:0). Increased levels of these odd-chain FA have been linked to dairy fat intake [84], including from low-fat dairy products [85]. A possible explanation for the increase in odd-chain PC is the patients dietary approach, which is based on a low-fat diet with frequent feeding. This frequent feeding could have led to a higher intake of dairy fat, resulting in the increased levels of odd-chain PC, which were previously identified in milk lipids [86]. However, there is still a lack of studies with FAOD patients that confirm this explanation for the increase in odd-chain lipid species. Also, an increase in PC 37:4 (PC 17:0_20:4) was previously observed in plasma samples from patients with VLCADD supplemented with MCT(either MCT-C8 or MCT-C7) [31]. Thus, elevated levels of odd-chain PC observed in long-chain patients, may be related either to intake of low-fat dairy products or to MCT supplementation prescribed to these patients.

Although the biological role of the up-regulation of Cer 41:2;O2 lipid species in LCHADD is still not fully known, ceramides have been identified as a key mediator of inflammation and death of neural and retinal pigment epithelium cells [87–89]. An increase in Cer lipid species has been also reported in neurodegenerative diseases [90]. Thus, the increase in Cer 41:2;O2 may be a risk factor for neurological and ophthalmic comorbidities in LCHADD patients (Table 2).

Regarding the clustering analysis of the top 50 of the most discriminant lipid species from the neutral lipids (glycerolipids and sterol lipids) (Fig. 5), LCHADD and VLCADD groups revealed a more similar variation in neutral lipids between FAOD groups under study, as observed in PCA (Fig. 4). Among the variations considering the top 50 of the neutral lipids (Table 1), increased levels of TG 42:1, TG 44:1, TG 44:2, TG 52:6, and TG 58:9 were previously observed in plasma of patients with MCADD [19], with the same FA composition identified in this work (Supplementary Table S1). Additionally, an up-regulation of TG 44:1, TG 52:6, and TG 58:9 was also reported in the plasma of LCHADD patients [26], but without determination of FA composition. The increase in these 3 TG lipid species in LCHADD patients was previously associated with the elongation of long-chain FA, which could be further incorporated into TG lipid species [26].

Considering the TG species with the same variation trend in long-chain FAOD (Table 2), only TG 46:3 has been previously reported to be increased in the plasma of LCHADD patients, but not related to a specific FA composition [26]. In this work, 3 distinct FA compositions were found for TG 46:3, as follows: TG 12:0_16:1_18:2, TG 14:0_14:1_18:2, and TG 14:1_14:1_18:1. The increase of FA 14:1 and FA 16:1 was previously observed for both long-chain FAOD [22,25]. Of note, 4 TG species (TG 49:0, TG 49:2, TG 51:0, TG 51:1 and TG 51:4) were esterified with odd-chain FA, such as FA 15:0 and FA 17:0. The increase in odd-chain TG, bearing these FA, could be related to the dietary intake specially of diary fat. as the dietary treatment followed by these patients based on frequent feeding [84]. The increase in TG 50:3 and TG 50:4 may have a cardioprotective effect in these patients, as these lipid species were associated with a decreased risk of cardiovascular disease [70,91] and long-chain FAOD could present cardiomyopathy (Table 2) [7,71]. Also, VLCADD patients exhibited an up-regulation of TG lipid species (TG 43:0, TG 45:0, TG 45:1, TG 45:2, TG 47:0, TG 47:1, TG 47:2, TG 49:1and TG 49:3) containing odd-chain FA (FA 15:0, FA 17:0 and FA 17:1), possibly due to dairy intake [84]. In addition, the increase in DG 36:4 (DG 16:0_20:4), observed in MCADD, is in line with the accumulation of FA 16:0 and FA 20:4 *n*-6, previously reported for

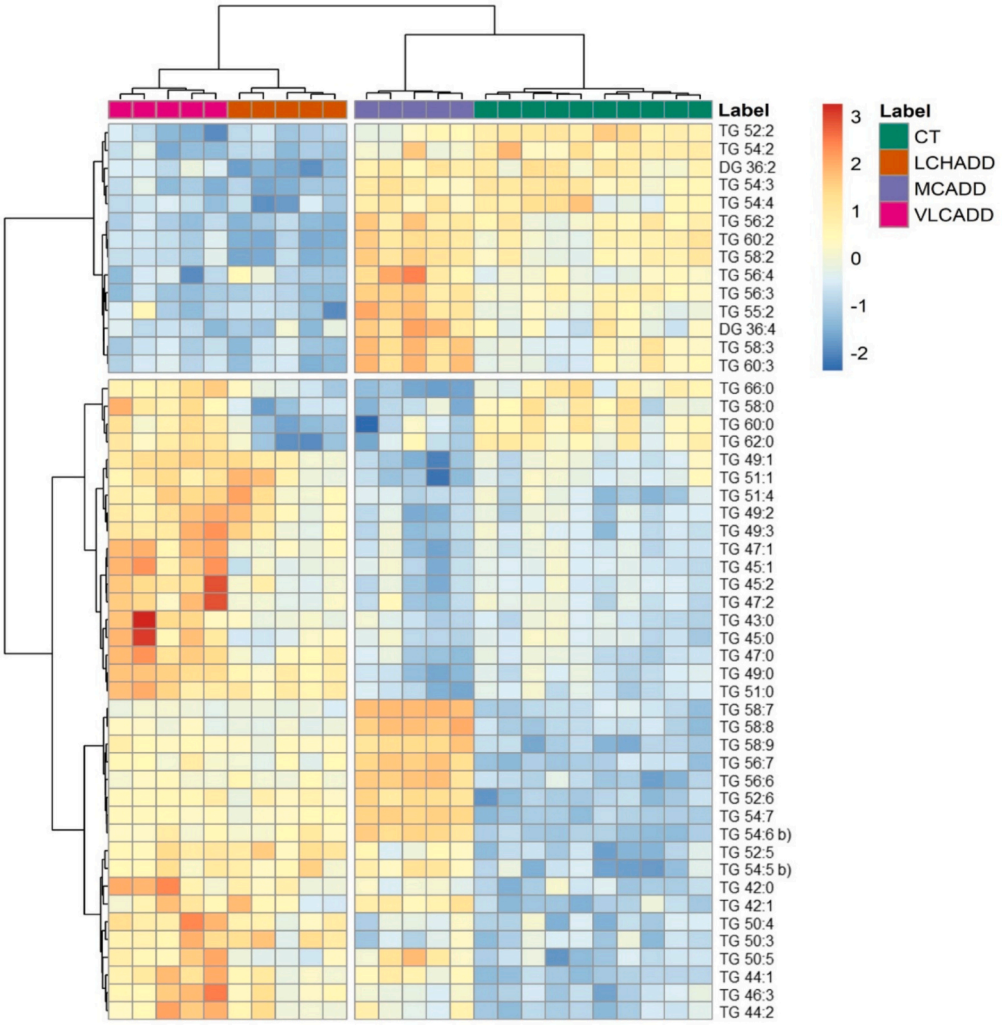

Fig. 5. Two-dimensional hierarchical clustering heatmap of the 50 most discriminative ($q < 0.001$) neutral lipid species among the CT, MCADD, LCHADD, and VLCADD groups. The relative abundance levels are shown on the red-yellow-blue scale, with numbers representing the fold difference from the overall mean. The red colour indicates high abundance, while blue indicates low abundance. Yellow represents null values. The clustering of the control and disease groups is represented by the dendrogram at the top, while the clustering of individual lipid species is represented by the dendrogram on the left. The lipid species are labelled as follows: AAAA xx:i (AAAA = lipid class abbreviation; xx = number of carbon atoms in FA; i = number of double bonds). The suffix "a" or "b" is used to differentiate isomers with distinct elution times. The abbreviations of lipid classes are as follows: DG, diacylglycerol; TG, triacylglycerol.

this disorder [19].

Our results with DBS samples highlighted specific alterations in lipid metabolites, such as glycerophospholipids, and glycerolipids, which may hold potential as biomarkers for FAOD prognosis. However, further longitudinal studies are needed to assess whether these lipid species are associated clinical outcomes, while accounting for age, treatment response, disease severity, and phenotypic variability. The possible association of the changes at the level of lipid species and the development of comorbidities, such as cardiomyopathy in long-chain FAOD, add further support to the importance of lipidomics studies in FAOD.

5. Conclusion

Our results revealed that FAOD (MCADD, LCHADD, and VLCADD) can significantly alter lipid metabolism, leading to specific changes in the whole blood lipid profile. Statistically significant alterations were observed in CAR, PC, LPC, PE, LPE, PI, SM, Cer, HexCer, TG, and DG lipid species. Particularly, increase levels of PC and LPC lipid species, together with decrease levels of PE and ether-linked PE lipid species were observed as common to all FAOD patients, making them potential biomarkers for FAOD prognosis. Additionally, lipid variations were identified as specific to each FAOD, and other lipid species revealed the same trend variation for long-chain FAOD (LCHADD and VLCADD). In MCADD patients it was observed a decreased in plasmenyl PC, which can be a possible contribution for reducing the oxidative stress already reported for MCADD. Also, the increase in Cer observed in LCHADD can play a role in neurodegenerative symptoms reported in this disorder. The increase in odd-chain TG observed for long-chain FAOD patients can be related to the MCT supplementation.

This work demonstrated that DBS samples are suitable for studying the lipidome plasticity in MCADD, LCHADD, and VLCADD. DBS revealed unique lipidomic profiles for FAOD, indicating changes in lipid metabolism and underscoring the possibility of lipidomics for disease surveillance.

CRediT authorship contribution statement

Inês M.S. Guerra: Visualization, Methodology, Investigation, Formal analysis, Conceptualization, Writing – review & editing, Writing – original draft. **Hugo Rocha:** Validation, Resources, Investigation, Writing – review & editing. **Sónia Moreira:** Validation, Investigation, Writing – review & editing. **Ana Gaspar:** Validation, Investigation,

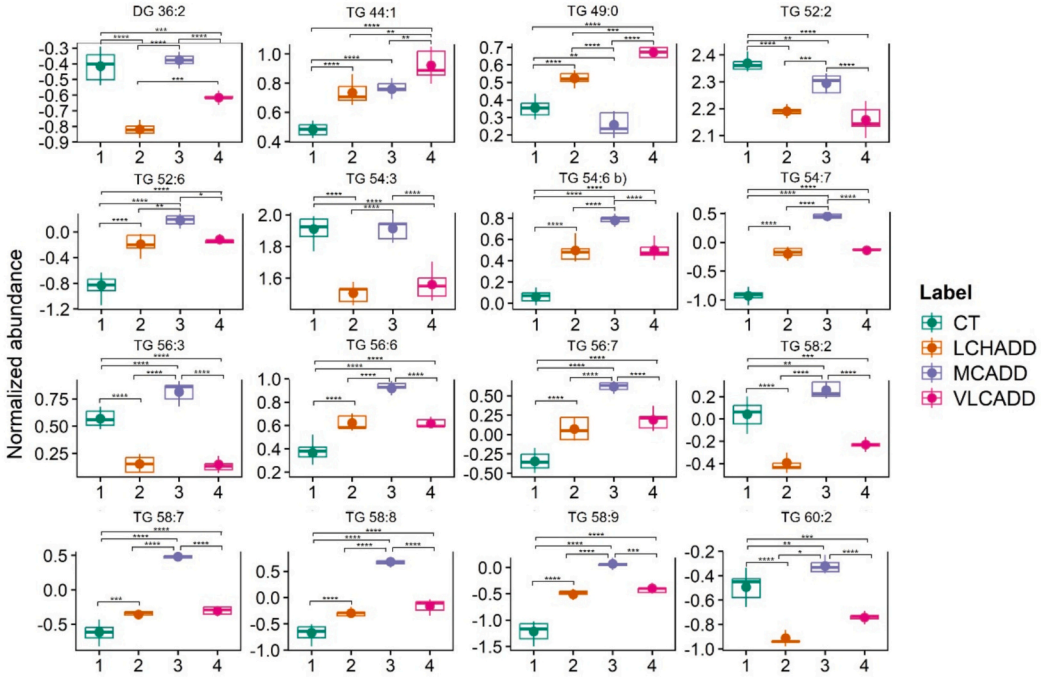

Fig. 6. Boxplots of the 16 most significant neutral lipid species identified through univariate analysis between control (CT), long-chain hydroxy acyl-CoA dehydrogenase deficiency (LCHADD), medium-chain acyl-CoA dehydrogenase deficiency (MCADD), and very long-chain acyl-CoA dehydrogenase deficiency (VLCADD) individuals. Significant differences between the groups are identified by horizontal lines and marked as follows: * $q < 0.05$, ** $q < 0.01$, *** $q < 0.001$ and **** $q < 0.0001$. The lipid species are labelled as follows: AAAA (xx:i) (AAAA = lipid class abbreviation; xx = the number of carbon atoms in FA(s); i = the number of double bonds). Abbreviations of the lipid classes: DG, diacylglycerol; TG, triacylglycerol.

Table 2
Mitochondrial fatty acid β-oxidation disorders (FAOD) under study and their acylcarnitine (CAR) markers, and clinical presentations/comorbidities. Adapted from Guerra *et al.* [3]. CAR lipid species highlighted in bold showed significant variations in this work.

Deficiency	Acylcarnitine markers	Clinical presentations/ comorbidities
Medium-chain acyl-CoA dehydrogenase deficiency (MCADD)	**CAR 8:0**, CAR8:0/ CAR10:0 and CAR8:0/ CAR2:0	Hypoketotic hypoglycemia, liver dysfunction, and encephalopathy
Very long-chain acyl-CoA dehydrogenase deficiency (VLCADD)	**CAR 14:1**, CAR 14:2, CAR 14:1/CAR 2:0 and CAR 14:1/CAR 12:1	Hypoketotic hypoglycemia, rhabdomyolysis, cardiomyopathy, skeletal myopathy, and liver dysfunction
Long-chain 3-hydroxyacyl-CoA dehydrogenase deficiency (LCHADD)	**CAR 16:0;O**, CAR 18:1;O and CAR 18:0; O	Hypoketotic hypoglycemia, rhabdomyolysis, cardiomyopathy, skeletal myopathy, liver dysfunction, peripherical neuropathy and retinopathy

Lipid class abbreviations: CAR, acylcarnitine. The lipid species are labelled as follows: AAAA xx:i (AAAA = lipid class abbreviation; xx = number of carbon atoms in FA; i = number of double bonds). The suffix 'O' indicates that the CAR lipid species is hydroxylated.

Writing – review & editing. **Ana C. Ferreira:** Validation, Investigation, Writing – review & editing. **Helena Santos:** Validation, Investigation, Writing – review & editing. **Esmeralda Rodrigues:** Validation, Investigation, Writing – review & editing. **Paulo Castro-Chaves:** Validation, Investigation, Writing – review & editing. **Tânia Melo:** Validation, Methodology, Investigation, Writing – review & editing. **Laura Goracci:** Visualization, Validation, Software, Formal analysis, Data curation, Writing – review & editing. **Pedro Domingues:** Visualization, Validation, Software, Methodology, Investigation, Formal analysis, Data curation, Writing – review & editing. **Ana S.P. Moreira:** Visualization, Validation, Supervision, Methodology, Investigation, Formal analysis, Data curation, Conceptualization, Writing – review & editing, Writing – original draft. **M. Rosário Domingues:** Visualization, Validation, Supervision, Investigation, Funding acquisition, Formal analysis, Data curation, Conceptualization, Writing – review & editing, Writing – original draft.

Declaration of competing interest

The authors declare that they have no known competing financial interests or personal relationships that could have appeared to influence the work reported in this paper.

Acknowledgments

The authors acknowledge to FCT/MCTES the financial support to CESAM (UID Centro de Estudos do Ambiente e Mar (CESAM) + LA/P/0094/2020) and LAQV/REQUIMTE (UID/50006 - Laboratório Associado para a Química Verde - Tecnologias e Processos Limpos) through national funds and, where applicable, co-financed by the FEDER, within the PT2020 Partnership Agreement and Compete 2020. Inês M. S. Guerra (2021.04754.BD; doi:10.54499/2021.04754.BD) is grateful to FCT for the PhD grant. Tânia Melo thanks the Junior Researcher contract in the scope of the Individual Call to Scientific Employment Stimulus 2020 (CEECIND/01578/2020; doi:10.54499/2020.01578.CEECIND/CP1589/CT0010). The authors are thankful to the COST Action EpiLipidNET, CA19105-Pan-European Network in Lipidomics and EpiLipidomics. The authors acknowledge Molecular Discovery Ltd. for the Lipostar version 2.1.5 license.

Appendix A. Supplementary data

Supplementary data to this article can be found online at https://doi.org/10.1016/j.bbalip.2025.159621.

Data availability

Data will be made available on request.

References

[1] K.G. Sim, J. Hammond, B. Wilcken, Strategies for the diagnosis of mitochondrial fatty acid β-oxidation disorders, Clin. Chim. Acta 323 (2002) 37–58, https://doi.org/10.1016/S0009-8981(02)00182-1.

[2] S.J.G. Knottnerus, J.C. Bleeker, R.C.I. Wüst, S. Ferdinandusse, L. Ijlst, F.A. Wijburg, R.J.A. Wanders, G. Visser, R.H. Houtkooper, Disorders of mitochondrial long-chain fatty acid oxidation and the carnitine shuttle, Rev. Endocr. Metab. Disord. 19 (2018) 93–106, https://doi.org/10.1007/s11154-018-9448-1.

[3] I.M.S. Guerra, H.B. Ferreira, T. Melo, H. Rocha, S. Moreira, L. Diogo, M. R. Domingues, A.S.P. Moreira, Mitochondrial fatty acid β-oxidation disorders: from disease to Lipidomic studies—a critical review, Int. J. Mol. Sci. 23 (2022) 13933, https://doi.org/10.3390/ijms232213933.

[4] G.S. Ribas, C.R. Vargas, Evidence that oxidative disbalance and mitochondrial dysfunction are involved in the pathophysiology of fatty acid oxidation disorders, Cell. Mol. Neurobiol. (2020), https://doi.org/10.1007/s10571-020-00955-7.

[5] P. Ruiz-Sala, L. Peña-Quintana, Biochemical markers for the diagnosis of mitochondrial fatty acid oxidation diseases, J. Clin. Med. 10 (2021) 4855, https://doi.org/10.3390/jcm10214855.

[6] J.L. Merritt, E. MacLeod, A. Jurecka, B. Hainline, Clinical manifestations and management of fatty acid oxidation disorders, Rev. Endocr. Metab. Disord. 21 (2020) 479–493, https://doi.org/10.1007/s11154-020-09568-3.

[7] Nenad Blau, C. Dionisi-Vici, R.Ferreira, Christine Vianey-Saban, Clara D. M. van Karnebeek, Physician's Guide to the Diagnosis, Treatment, and Follow-Up of Inherited Metabolic Diseases, 2nd ed., Springer Cham, n.d. https://doi.org/10.1007/978-3-030-67727-5 (accessed August 16, 2022).

[8] U. Spiekerkoetter, B. Sun, T. Zytkovicz, R. Wanders, A.W. Strauss, U. Wendel, MS/MS-based newborn and family screening detects asymptomatic patients with very-long-chain acyl-CoA dehydrogenase deficiency, J. Pediatr. 143 (2003) 335–342, https://doi.org/10.1067/S0022-3476(03)00292-0.

[9] K. Maclean, V.S. Rasiah, E.P.E. Kirk, K. Carpenter, S. Cooper, K. Lui, J. Oei, Pulmonary haemorrhage and cardiac dysfunction in a neonate with medium-chain acyl-CoA dehydrogenase (MCAD) deficiency, Acta Paediatr. 94 (2005) 114–116, https://doi.org/10.1111/j.1651-2227.2005.tb01797.x.

[10] J.R. Wiles, N. Leslie, T.K. Knilans, H. Akinbi, Prolonged QTc interval in association with medium-chain acyl-coenzyme a dehydrogenase deficiency, Pediatrics 133 (2014) e1781–e1786, https://doi.org/10.1542/peds.2013-1105.

[11] T.F. Lang, Adult presentations of medium-chain acyl-CoA dehydrogenase deficiency (MCADD), J. Inherit. Metab. Dis. 32 (2009) 675–683, https://doi.org/10.1007/s10545-009-1202-0.

[12] F. Feillet, G. Steinmann, C. Vianey-Saban, C. de Chillou, N. Sadoul, E. Lefebvre, M. Vidailhet, P.E. Bollaert, Adult presentation of MCAD deficiency revealed by coma and severe arrythmias, Intensive Care Med. 29 (2003) 1594–1597, https://doi.org/10.1007/s00134-003-1871-3.

[13] J.L. Merritt, I.J. Chang, Medium-chain acyl-coenzyme A dehydrogenase deficiency, in: M.P. Adam, G.M. Mirzaa, R.A. Pagon, S.E. Wallace, L.J. Bean, K.W. Gripp, A. Amemiya (Eds.), GeneReviews®, University of Washington, Seattle, Seattle (WA), 2000. http://www.ncbi.nlm.nih.gov/books/NBK1424/ (accessed April 18, 2023).

[14] S.J. Mayell, L. Edwards, F.E. Reynolds, A.B. Chakrapani, Late presentation of medium-chain acyl-CoA dehydrogenase deficiency, J. Inherit. Metab. Dis. 30 (2007) 104, https://doi.org/10.1007/s10545-006-0488-4.

[15] J. Baruteau, P. Sachs, P. Broué, M. Brivet, H. Abdoul, C. Vianey-Saban, H. Ogier de Baulny, Clinical and biological features at diagnosis in mitochondrial fatty acid beta-oxidation defects: a French pediatric study of 187 patients, J. Inherit. Metab. Dis. 36 (2013) 795–803, https://doi.org/10.1007/s10545-012-9542-6.

[16] S. Tucci, An altered sphingolipid profile as a risk factor for progressive neurodegeneration in long-chain 3-Hydroxyacyl-CoA deficiency (LCHADD), Int. J. Mol. Sci. 23 (2022) 7144, https://doi.org/10.3390/ijms23137144.

[17] R.J.A. Wanders, G. Visser, S. Ferdinandusse, F.M. Vaz, R.H. Houtkooper, Mitochondrial fatty acid oxidation disorders: laboratory diagnosis, pathogenesis, and the complicated route to treatment, Journal of Lipid and Atherosclerosis 9 (2020) 313–333, https://doi.org/10.12997/jla.2020.9.3.313.

[18] E. Mason, C.C.T. Hindmarch, K.J. Dunham-Snary, Medium-chain acyl-COA dehydrogenase deficiency: pathogenesis, diagnosis, and treatment, Endocrinology, Diabetes & Metabolism 6 (2023) e385, https://doi.org/10.1002/edm2.385.

[19] I.M.S. Guerra, H.B. Ferreira, T. Maurício, M. Pinho, L. Diogo, S. Moreira, L. Goracci, S. Bonciarelli, T. Melo, P. Domingues, M.R. Domingues, A.S.P. Moreira, Plasma lipidomics analysis reveals altered profile of triglycerides and phospholipids in children with medium-chain acyl-CoA dehydrogenase deficiency, J. Inherited Metab. Dis. n/a (n.d.). doi:https://doi.org/10.1002/jimd.12718.

[20] J.L.K. Van Hove, S.G. Kahler, M.D. Feezor, J.P. Ramakrishna, P. Hart, W.R. Treem, J.-J. Shen, D. Matern, D.S. Millington, Acylcarnitines in plasma and blood spots of patients with long-chain 3-hydroxyacyl-coenzyme a dehydrogenase defiency, J. Inherit. Metab. Dis. 23 (2000) 571–582, https://doi.org/10.1023/A:1005673828469.

[21] L. Najdekr, A. Gardlo, L. Mádrová, D. Friedecký, H. Janečková, E.S. Correa, R. Goodacre, T. Adam, Oxidized phosphatidylcholines suggest oxidative stress in patients with medium-chain acyl-CoA dehydrogenase deficiency, Talanta 139 (2015) 62–66, https://doi.org/10.1016/j.talanta.2015.02.041.

[22] G. Martínez, G. Jiménez-Sánchez, P. Divry, C. Vianey-Saban, E. Riudor, M. Rodés, P. Briones, A. Ribes, Plasma free fatty acids in mitochondrial fatty acid oxidation defects, Clin. Chim. Acta 267 (1997) 143–154, https://doi.org/10.1016/S0009-8981(97)00130-7.

[23] C.G. Costa, L. Dorland, U. Holwerda, I. Tavares de Almeida, B.-T. Poll-The, C. Jakobs, M. Duran, Simultaneous analysis of plasma free fatty acids and their 3-hydroxy analogs in fatty acid β-oxidation disorders, Clin. Chem. 44 (1998) 463–471, https://doi.org/10.1093/clinchem/44.3.463.

[24] M. Kimura, H.R. Yoon, P. Wasant, Y. Takahashi, S. Yamaguchi, A sensitive and simplified method to analyze free fatty acids in children with mitochondrial beta oxidation disorders using gas chromatography/mass spectrometry and dried blood spots, Clin. Chim. Acta 316 (2002) 117–121, https://doi.org/10.1016/S0009-8981(01)00741-0.

[25] W. Onkenhout, V. Venizelos, H.R. Scholte, J.B.C. de Klerk, B.J.H.M. Poorthuis, Intermediates of unsaturated fatty acid oxidation are incorporated in triglycerides but not in phospholipids in tissues from patients with mitochondrial β-oxidation defects, J. Inherit. Metab. Dis. 24 (2001) 337–344, https://doi.org/10.1023/A:1010592232317.

[26] C.S. McCoin, B.D. Piccolo, T.A. Knotts, D. Matern, J. Vockley, M.B. Gillingham, S. H. Adams, Unique plasma metabolomic signatures of individuals with inherited disorders of long-chain fatty acid oxidation, J. Inherit. Metab. Dis. 39 (2016) 399–408, https://doi.org/10.1007/s10545-016-9915-3.

[27] J.J. Shen, D. Matern, D.S. Millington, S. Hillman, M.D. Feezor, M.J. Bennett, M. Qumsiyeh, S.G. Kahler, Y.-T. Chen, J.L.K. Van Hove, Acylcarnitines in fibroblasts of patients with long-chain 3-hydroxyacyl-CoA dehydrogenase deficiency and other fatty acid oxidation disorders, J. Inherit. Metab. Dis. 23 (2000) 27–44, https://doi.org/10.1023/A:1005694712583.

[28] K.I. Alatibi, J. Hagenbuchner, Z. Wehbe, D. Karall, M.J. Ausserlechner, J. Vockley, U. Spiekerkoetter, S.C. Grünert, S. Tucci, Different lipid signature in fibroblasts of long-chain fatty acid oxidation disorders, Cells 10 (2021) 1239, https://doi.org/10.3390/cells10051239.

[29] K.I. Alatibi, S. Tholen, Z. Wehbe, J. Hagenbuchner, D. Karall, M.J. Ausserlechner, O. Schilling, S.C. Grünert, J. Vockley, S. Tucci, Lipidomic and proteomic alterations induced by even and odd medium-chain fatty acids on fibroblasts of long-chain fatty acid oxidation disorders, Int. J. Mol. Sci. 22 (2021) 10556, https://doi.org/10.3390/ijms221910556.

[30] S. Tucci, S. Behringer, U. Spiekerkoetter, De novo fatty acid biosynthesis and elongation in very long-chain acyl-CoA dehydrogenase-deficient mice supplemented with odd or even medium-chain fatty acids, FEBS J. 282 (2015) 4242–4253, https://doi.org/10.1111/febs.13418.

[31] E. Sklirou, A.N. Alodaib, S.F. Dobrowolski, A.-W.A. Mohsen, J. Vockley, Physiological perspectives on the use of Triheptanoin as Anaplerotic therapy for long chain fatty acid oxidation disorders, Front. Genet. 11 (2021), https://doi.org/10.3389/fgene.2020.598760.

[32] M. Schwantje, S. Mosegaard, S.J.G. Knottnerus, J.B. van Klinken, R.J. Wanders, H. van Lenthe, J. Hermans, L. Ijlst, S.W. Denis, Y.R.J. Jaspers, S.A. Fuchs, R. H. Houtkooper, S. Ferdinandusse, F.M. Vaz, Tracer-based lipidomics enables the discovery of disease-specific candidate biomarkers in mitochondrial β-oxidation disorders, FASEB J. 38 (2024) e23478, https://doi.org/10.1096/fj.202302163R.

[33] R. Sebaa, R.H. AlMalki, W. Alseraty, A.M. Abdel Rahman, A distinctive metabolomics profile and potential biomarkers for very long acylcarnitine dehydrogenase deficiency (VLCADD) diagnosis in newborns, Metabolites 13 (2023) 725, https://doi.org/10.3390/metabo13060725.

[34] R. Sebaa, M. AlMogren, W. Alseraty, A.M. Abdel Rahman, Untargeted metabolomics identifies biomarkers for MCADD neonates in dried blood spots, Int. J. Mol. Sci. 24 (2023) 9657, https://doi.org/10.3390/ijms24119657.

[35] A.M. Lund, M.A. Dixon, P. Vreken, J.V. Leonard, A.A.M. Morris, Plasma and erythrocyte fatty acid concentrations in long-chain 3-hydroxyacyl-CoA dehydrogenase deficiency, J. Inherit. Metab. Dis. 26 (2003) 410–412, https://doi.org/10.1023/A:1025175606891.

[36] K. Czubowicz, H. Jęśko, P. Wencel, W.J. Lukiw, R.P. Strosznajder, The role of ceramide and Sphingosine-1-phosphate in Alzheimer's disease and other neurodegenerative disorders, Mol. Neurobiol. 56 (2019) 5436–5455, https://doi.org/10.1007/s12035-018-1448-3.

[37] E. Rockenstein, J. Clarke, C. Viel, N. Panarello, C.M. Treleaven, C. Kim, B. Spencer, A. Adame, H. Park, J.C. Dodge, S.H. Cheng, L.S. Shihabuddin, E. Masliah, S. P. Sardi, Glucocerebrosidase modulates cognitive and motor activities in murine models of Parkinson's disease, Hum. Mol. Genet. 25 (2016) 2645–2660, https://doi.org/10.1093/hmg/ddw124.

[38] G. Liebisch, E. Fahy, J. Aoki, E.A. Dennis, T. Durand, C.S. Ejsing, M. Fedorova, I. Feussner, W.J. Griffiths, H. Köfeler, A.H. Merrill, R.C. Murphy, V.B. O'Donnell, O. Oskolkova, S. Subramaniam, M.J.O. Wakelam, F. Spener, Update on LIPID MAPS classification, nomenclature, and shorthand notation for MS-derived lipid structures, J. Lipid Res. 61 (2020) 1539–1555, https://doi.org/10.1194/jlr.S120001025.

[39] E. Fahy, S. Subramaniam, R.C. Murphy, M. Nishijima, C.R.H. Raetz, T. Shimizu, F. Spener, G. van Meer, M.J.O. Wakelam, E.A. Dennis, Update of the LIPID MAPS comprehensive classification system for lipids1, J. Lipid Res. 50 (2009) S9–S14, https://doi.org/10.1194/jlr.R800095-JLR200.

[40] E. Fahy, S. Subramaniam, H.A. Brown, C.K. Glass, A.H. Merrill, R.C. Murphy, C.R. H. Raetz, D.W. Russell, Y. Seyama, W. Shaw, T. Shimizu, F. Spener, G. van Meer, M. S. VanNieuwenhze, S.H. White, J.L. Witztum, E.A. Dennis, A comprehensive classification system for lipids1, J. Lipid Res. 46 (2005) 839–861, https://doi.org/10.1194/jlr.E400004-JLR200.

[41] M.A. Alves, S. Lamichhane, A. Dickens, A. McGlinchey, H.C. Ribeiro, P. Sen, F. Wei, T. Hyötyläinen, M. Orešič, Systems biology approaches to study lipidomes in health

and disease, Biochim. Biophys. Acta (BBA) – Mol. Cell Biol. Lipids 2021 (1866) 158857, https://doi.org/10.1016/j.bbalip.2020.158857.
[42] F. Wei, S. Lamichhane, M. Orešič, T. Hyötyläinen, Lipidomes in health and disease: analytical strategies and considerations, TrAC Trends Anal. Chem. 120 (2019) 115664, https://doi.org/10.1016/j.trac.2019.115664.
[43] M.U. Thangavelu, B. Wouters, A. Kindt, I.K.M. Reiss, T. Hankemeier, Blood microsampling technologies: innovations and applications in 2022, Anal Sci Adv 4 (2023) 154–180, https://doi.org/10.1002/ansa.202300011.
[44] H.B. Ferreira, I.M.S. Guerra, T. Melo, H. Rocha, A.S.P. Moreira, A. Paiva, M. R. Domingues, Dried blood spots in clinical lipidomics: optimization and recent findings, Anal. Bioanal. Chem. 414 (2022) 7085–7101, https://doi.org/10.1007/s00216-022-04221-1.
[45] E.G. Bligh, W.J. Dyer, A rapid method of total lipid extraction and purification, Can. J. Biochem. Physiol. 37 (1959) 911–917, https://doi.org/10.1139/o59-099.
[46] E.M. Bartlett, D.H. Lewis, Spectrophotometric determination of phosphate esters in the presence and absence of orthophosphate, Anal. Biochem. 36 (1970) 159–167, https://doi.org/10.1016/0003-2697(70)90343-X.
[47] G.W. Chapman, A conversion factor to determine phospholipid content in soybean and sunflower crude oils, J. Am. Oil Chem. Soc. 57 (1980) 299–302, https://doi.org/10.1007/BF02662211.
[48] R: The R Project for Statistical Computing, (n.d.). https://www.r-project.org/ (accessed July 18, 2024).
[49] RStudio|Open source & professional software for data scienceteams, Posit (n.d.). https://rstudio.com/ (accessed July 18, 2024).
[50] J. Xia, D.S. Wishart, Using MetaboAnalyst 3.0 for comprehensive metabolomics data analysis, Curr. Protoc. Bioinformatics 55 (2016), https://doi.org/10.1002/cpbi.11, 14.10.1-14.10.91.
[51] Y.V. Karpievitch, S.B. Nikolic, R. Wilson, J.E. Sharman, L.M. Edwards, Metabolomics data normalization with EigenMS, PloS One 9 (2014) e116221, https://doi.org/10.1371/journal.pone.0116221.
[52] FactoMineR: Multivariate Exploratory Data Analysis and Data Mining version 2.11 from CRAN, (n.d.). https://rdrr.io/cran/FactoMineR/ (accessed July 18, 2024).
[53] factoextra: Extract and Visualize the Results of Multivariate Data Analyses version 1.0.7 from CRAN, (n.d.). https://rdrr.io/cran/factoextra/ (accessed July 18, 2024).
[54] pheatmap: Pretty Heatmaps version 1.0.12 from CRAN, (n.d.). https://rdrr.io/cran/pheatmap/ (accessed July 18, 2024).
[55] rstatix: Pipe-Friendly Framework for Basic Statistical Tests version 0.7.2 from CRAN, (n.d.). https://rdrr.io/cran/rstatix/ (accessed July 18, 2024).
[56] Create Elegant Data Visualisations Using the Grammar of Graphics, (n.d.). https://ggplot2.tidyverse.org/ (accessed July 18, 2024).
[57] A.A.M. Morris, U. Spiekerkoetter, Disorders of mitochondrial fatty acid oxidation & riboflavin metabolism, in: J.-M. Saudubray, M.R. Baumgartner, J. Walter (Eds.), Inborn Metabolic Diseases: Diagnosis and Treatment, Springer, Berlin, Heidelberg, 2016, pp. 201–213, https://doi.org/10.1007/978-3-662-49771-5_12.
[58] U. Spiekerkoetter, M. Lindner, R. Santer, M. Grotzke, M.R. Baumgartner, H. Boehles, A. Das, C. Haase, J.B. Hennermann, D. Karall, H. de Klerk, I. Knerr, H. G. Koch, B. Plecko, W. Röschinger, K.O. Schwab, D. Scheible, F.A. Wijburg, J. Zschocke, E. Mayatepek, U. Wendel, Treatment recommendations in long-chain fatty acid oxidation defects: consensus from a workshop, J. Inherit. Metab. Dis. 32 (2009) 498–505, https://doi.org/10.1007/s10545-009-1126-8.
[59] V. Rovelli, F. Manzoni, K. Viau, M. Pasquali, N. Longo, Clinical and biochemical outcome of patients with very long-chain acyl-CoA dehydrogenase deficiency, Mol. Genet. Metab. 127 (2019) 64–73, https://doi.org/10.1016/j.ymgme.2019.04.001.
[60] M. Kompare, W.B. Rizzo, Mitochondrial fatty-acid oxidation disorders, Semin. Pediatr. Neurol. 15 (2008) 140–149, https://doi.org/10.1016/j.spen.2008.05.008.
[61] S. Wallner, G. Schmitz, Plasmalogens the neglected regulatory and scavenging lipid species, Chem. Phys. Lipids 164 (2011) 573–589, https://doi.org/10.1016/j.chemphyslip.2011.06.008.
[62] J. Leßig, B. Fuchs, Plasmalogens in biological systems: their role in oxidative processes in biological membranes, their contribution to pathological processes and aging and plasmalogen analysis, Curr. Med. Chem. 16 (n.d.) 2021–2041.
[63] R.A. Zoeller, A.C. Lake, N. Nagan, D.P. Gaposchkin, M.A. Legner, W. Lieberthal, Plasmalogens as endogenous antioxidants: somatic cell mutants reveal the importance of the vinyl ether, Biochem. J. 338 (1999) 769–776.
[64] P.F. Schuck, P.C. Ceolato, G.C. Ferreira, A. Tonin, G. Leipnitz, C.S. Dutra-Filho, A. Latini, M. Wajner, Oxidative stress induction by cis-4-decenoic acid: relevance for MCAD deficiency, Free Radic. Res. (2007), https://doi.org/10.1080/10715760701687109.
[65] A.M. Tonin, M. Grings, E.N.B. Busanello, A.P. Moura, G.C. Ferreira, C.M. Viegas, C. G. Fernandes, P.F. Schuck, M. Wajner, Long-chain 3-hydroxy fatty acids accumulating in LCHAD and MTP deficiencies induce oxidative stress in rat brain, Neurochem. Int. 56 (2010) 930–936, https://doi.org/10.1016/j.neuint.2010.03.025.
[66] B. Seminotti, G. Leipnitz, A. Karunanidhi, C. Kochersperger, V.Y. Roginskaya, S. Basu, Y. Wang, P. Wipf, B. Van Houten, A.-W. Mohsen, J. Vockley, Mitochondrial energetics is impaired in very long-chain acyl-CoA dehydrogenase deficiency and can be rescued by treatment with mitochondria-targeted electron scavengers, Hum. Mol. Genet. 28 (2019) 928–941, https://doi.org/10.1093/hmg/ddy403.
[67] J.N. van der Veen, J.P. Kennelly, S. Wan, J.E. Vance, D.E. Vance, R.L. Jacobs, The critical role of phosphatidylcholine and phosphatidylethanolamine metabolism in health and disease, Biochim. Biophys. Acta Biomembr. 1859 (2017) 1558–1572, https://doi.org/10.1016/j.bbamem.2017.04.006.
[68] E. Toledo, C. Wittenbecher, C. Razquin, M. Ruiz-Canela, C.B. Clish, L. Liang, A. Alonso, P. Hernández-Alonso, N. Becerra-Tomás, F. Arós-Borau, D. Corella, E. Ros, R. Estruch, A. García-Rodríguez, M. Fitó, J. Lapetra, M. Fiol, Á.M. Alonso-Gomez, L. Serra-Majem, A. Deik, J. Salas-Salvadó, F.B. Hu, M.A. Martínez-González, Plasma lipidome and risk of atrial fibrillation: results from the PREDIMED trial, J. Physiol. Biochem. 79 (2023) 355–364, https://doi.org/10.1007/s13105-023-00958-0.
[69] S. Ranjbarvaziri, K.B. Kooiker, M. Ellenberger, G. Fajardo, M. Zhao, A.S. Vander Roest, R.A. Woldeyes, T.T. Koyano, R. Fong, N. Ma, L. Tian, G.M. Traber, F. Chan, J. Perrino, S. Reddy, W. Chiu, J.C. Wu, J.Y. Woo, K.M. Ruppel, J.A. Spudich, M. P. Snyder, K. Contrepois, D. Bernstein, Altered cardiac energetics and mitochondrial dysfunction in hypertrophic cardiomyopathy, Circulation 144 (2021) 1714–1731, https://doi.org/10.1161/CIRCULATIONAHA.121.053575.
[70] S.O. Diaz, J.L. Sánchez-Quesada, V. de Freitas, A. Leite-Moreira, A.S. Barros, A. Reis, Exploratory analysis of large-scale lipidome in large cohorts: are we any closer of finding lipid-based markers suitable for CVD risk stratification and management? Anal. Chim. Acta 1142 (2021) 189–200, https://doi.org/10.1016/j.aca.2020.10.037.
[71] U. Spiekerkoetter, B. Sun, T. Zytkovicz, R. Wanders, A.W. Strauss, U. Wendel, MS/MS-based newborn and family screening detects asymptomatic patients with very-long-chain acyl-CoA dehydrogenase deficiency, J. Pediatr. 143 (2003) 335–342, https://doi.org/10.1067/S0022-3476(03)00292-0.
[72] L.S. Huang, N.D. Hung, D.-E. Sok, M.R. Kim, Lysophosphatidylcholine containing docosahexaenoic acid at the sn-1 position is anti-inflammatory, Lipids 45 (2010) 225–236, https://doi.org/10.1007/s11745-010-3392-5.
[73] N.E. Braverman, A.B. Moser, Functions of plasmalogen lipids in health and disease, Biochim. Biophys. Acta (BBA) - Mol. Basis Dis. 1822 (2012) 1442–1452, https://doi.org/10.1016/j.bbadis.2012.05.008.
[74] J. Leßig, J. Schiller, J. Arnhold, B. Fuchs, Hypochlorous acid-mediated generation of glycerophosphocholine from unsaturated plasmalogen glycerophosphocholine lipids, J. Lipid Res. 48 (2007) 1316–1324, https://doi.org/10.1194/jlr.M600478-JLR200.
[75] D. Reis de Assis, R. de C. Maria, R. Borba Rosa, P.F. Schuck, C.A.J. Ribeiro, G. da Costa Ferreira, C.S. Dutra-Filho, A. Terezinha de Souza Wyse, C.M. Duval Wannmacher, M.L. Santos Perry, M. Wajner, Inhibition of energy metabolism in cerebral cortex of young rats by the medium-chain fatty acids accumulating in MCAD deficiency, Brain Res. 1030 (2004) 141–151, https://doi.org/10.1016/j.brainres.2004.10.010.
[76] A.U. Amaral, C. Cecatto, J.C. da Silva, A. Wajner, K. dos S. Godoy, R.T. Ribeiro, M. Wajner, cis-4-Decenoic and decanoic acids impair mitochondrial energy, redox and Ca2 + homeostasis and induce mitochondrial permeability transition pore opening in rat brain and liver: Possible implications for the pathogenesis of MCAD deficiency, Biochim. Biophys. Acta (BBA) – Bioenerg. 1857 (2016) 1363–1372, https://doi.org/10.1016/j.bbabio.2016.05.007.
[77] G. Scaini, K.R. Simon, A.M. Tonin, E.N.B. Busanello, A.P. Moura, G.C. Ferreira, M. Wajner, E.L. Streck, P.F. Schuck, Toxicity of octanoate and decanoate in rat peripheral tissues: evidence of bioenergetic dysfunction and oxidative damage induction in liver and skeletal muscle, Mol. Cell. Biochem. 361 (2012) 329–335, https://doi.org/10.1007/s11010-011-1119-4.
[78] A.M. Tonin, M. Grings, L.A. Knebel, Â. Zanatta, A.P. Moura, C.A.J. Ribeiro, G. Leipnitz, M. Wajner, Disruption of redox homeostasis in cerebral cortex of developing rats by acylcarnitines accumulating in medium-chain acyl-CoA dehydrogenase deficiency, Int. J. Dev. Neurosci. 30 (2012) 383–390, https://doi.org/10.1016/j.ijdevneu.2012.03.238.
[79] I.B. King, R.N. Lemaitre, M. Kestin, Effect of a low-fat diet on fatty acid composition in red cells, plasma phospholipids, and cholesterol esters: investigation of a biomarker of total fat intake2, Am. J. Clin. Nutr. 83 (2006) 227–236, https://doi.org/10.1093/ajcn/83.2.227.
[80] J. Whelan, K. Fritsche, Linoleic Acid, Adv. Nutr. 4 (2013) 311–312, https://doi.org/10.3945/an.113.003772.
[81] M. Mititelu, D. Lupuliasa, S.M. Neacșu, G. Olteanu, Ștefan S. Busnatu, A. Mihai, V. Popovici, N. Măru, S.C. Boroghină, S. Mihai, C.-B. Ioniță-Mîndrican, A. Scafa-Udriște, Polyunsaturated fatty acids and human health: a key to modern nutritional balance in association with polyphenolic compounds from food sources, Foods 14 (2025) 46, https://doi.org/10.3390/foods14010046.
[82] Q. Mao, Y. Kong, Effect of diet low in omega-6 polyunsaturated fatty acids on the global burden of cardiovascular diseases and future trends: evidence from the global burden of disease 2021, Front. Med. 11 (2025), https://doi.org/10.3389/fmed.2024.1485695.
[83] G. Rassias, M. Kestin, P.J. Nestel, Linoleic acid lowers LDL cholesterol without a proportionate displacement of saturated fatty acid, Eur. J. Clin. Nutr. 45 (1991) 315–320.
[84] L. Sellem, K.G. Jackson, L. Paper, I.D. Givens, J.A. Lovegrove, Can individual fatty acids be used as functional biomarkers of dairy fat consumption in relation to cardiometabolic health? A narrative review, Br. J. Nutr. 128 (n.d.) 2373–2386. doi: https://doi.org/10.1017/S0007114522000289.
[85] V. Albani, C. Celis-Morales, C.F.M. Marsaux, H. Forster, C.B. O'Donovan, C. Woolhead, A.L. Macready, R. Fallaize, S. Navas-Carretero, R. San-Cristobal, S. Kolossa, C. Mavrogianni, C.P. Lambrinou, G. Moschonis, M. Godlewska, A. Surwiłło, T.E. Gundersen, S.E. Kaland, Y. Manios, I. Traczyk, C.A. Drevon, E. R. Gibney, M.C. Walsh, J.A. Martinez, W.H.M. Saris, H. Daniel, J.A. Lovegrove, M. J. Gibney, A.J. Adamson, J.C. Mathers, L. Brennan, on behalf of the F. Study, Exploring the association of dairy product intake with the fatty acids C15:0 and C17:0 measured from dried blood spots in a multipopulation cohort: findings from the Food4Me study, Mol. Nutr. Food Res. 60 (2016) 834–845, https://doi.org/10.1002/mnfr.201500483.
[86] Z. Liu, C. Li, J. Pryce, S. Rochfort, Comprehensive characterization of bovine Milk lipids: phospholipids, sphingolipids, glycolipids, and ceramides, J. Agric. Food Chem. 68 (2020) 6726–6738, https://doi.org/10.1021/acs.jafc.0c01604.

[87] N. Sanvicens, T.G. Cotter, Ceramide is the key mediator of oxidative stress-induced apoptosis in retinal photoreceptor cells, J. Neurochem. 98 (2006) 1432–1444, https://doi.org/10.1111/j.1471-4159.2006.03977.x.
[88] I. Piano, E. Novelli, P. Gasco, R. Ghidoni, E. Strettoi, C. Gargini, Cone survival and preservation of visual acuity in an animal model of retinal degeneration, Eur. J. Neurosci. 37 (2013) 1853–1862, https://doi.org/10.1111/ejn.12196.
[89] M.V. Simon, S.K. Basu, B. Qaladize, R. Grambergs, N.P. Rotstein, N. Mandal, Sphingolipids as critical players in retinal physiology and pathology, J. Lipid Res. 62 (2021) 100037, https://doi.org/10.1194/jlr.TR120000972.
[90] L.M. Pujol-Lereis, Alteration of sphingolipids in biofluids: implications for neurodegenerative diseases, Int. J. Mol. Sci. 20 (2019) 3564, https://doi.org/10.3390/ijms20143564.
[91] C. Fernandez, M. Sandin, J.L. Sampaio, P. Almgren, K. Narkiewicz, M. Hoffmann, T. Hedner, B. Wahlstrand, K. Simons, A. Shevchenko, P. James, O. Melander, Plasma lipid composition and risk of developing cardiovascular disease, PloS One 8 (2013) e71846, https://doi.org/10.1371/journal.pone.0071846.